

Broadband dielectric behavior of MIL-100 metal-organic framework as a function of structural amorphization

Arun Singh Babal,^a Barbara E. Souza,^a Annika F. Möslein,^a Mario Gutiérrez,^a

Mark D. Frogley,^b and Jin-Chong Tan^{a,*}

^aMultifunctional Materials and Composites (MMC) Laboratory, Department of Engineering Science, University of Oxford, Parks Road, Oxford, OX1 3PJ, United Kingdom

^bDiamond Light Source, Harwell Campus, Chilton, Oxford, OX11 0DE, United Kingdom

*E-mail: jin-chong.tan@eng.ox.ac.uk

Contents

1. Powder X-ray diffraction (XRD).....	3
2. Fourier-transform infrared spectroscopy (ATR-FTIR).....	4
3. Thermogravimetric analysis (TGA).....	6
4. Dielectric properties.....	7
4.1 Basolite F300	7
4.1.1 Real Part of Dielectric Constant (ϵ').....	7
4.1.2 Imaginary Part of Dielectric Constant (ϵ'')	10
4.1.3 Dielectric Loss ($\tan \delta$).....	13
4.2 MIL-100-MG	16
4.2.1 Real Part of Dielectric Constant	16
4.2.2 Imaginary Part of Dielectric Constant.....	19
4.2.3 Dielectric Loss.....	22
4.3 Comparative dielectric loss.....	25
5. Reflectivity spectra $R(\omega)$ in the far-IR and mid-IR regions.....	26
6. Refractive index in THz region	27
7. The imaginary part of dielectric constant in the THz region.....	28
8. AC conductivity.....	29
8.1 Basolite F300	29
8.2 MIL-100-MG	32

1. Powder X-ray diffraction (XRD)

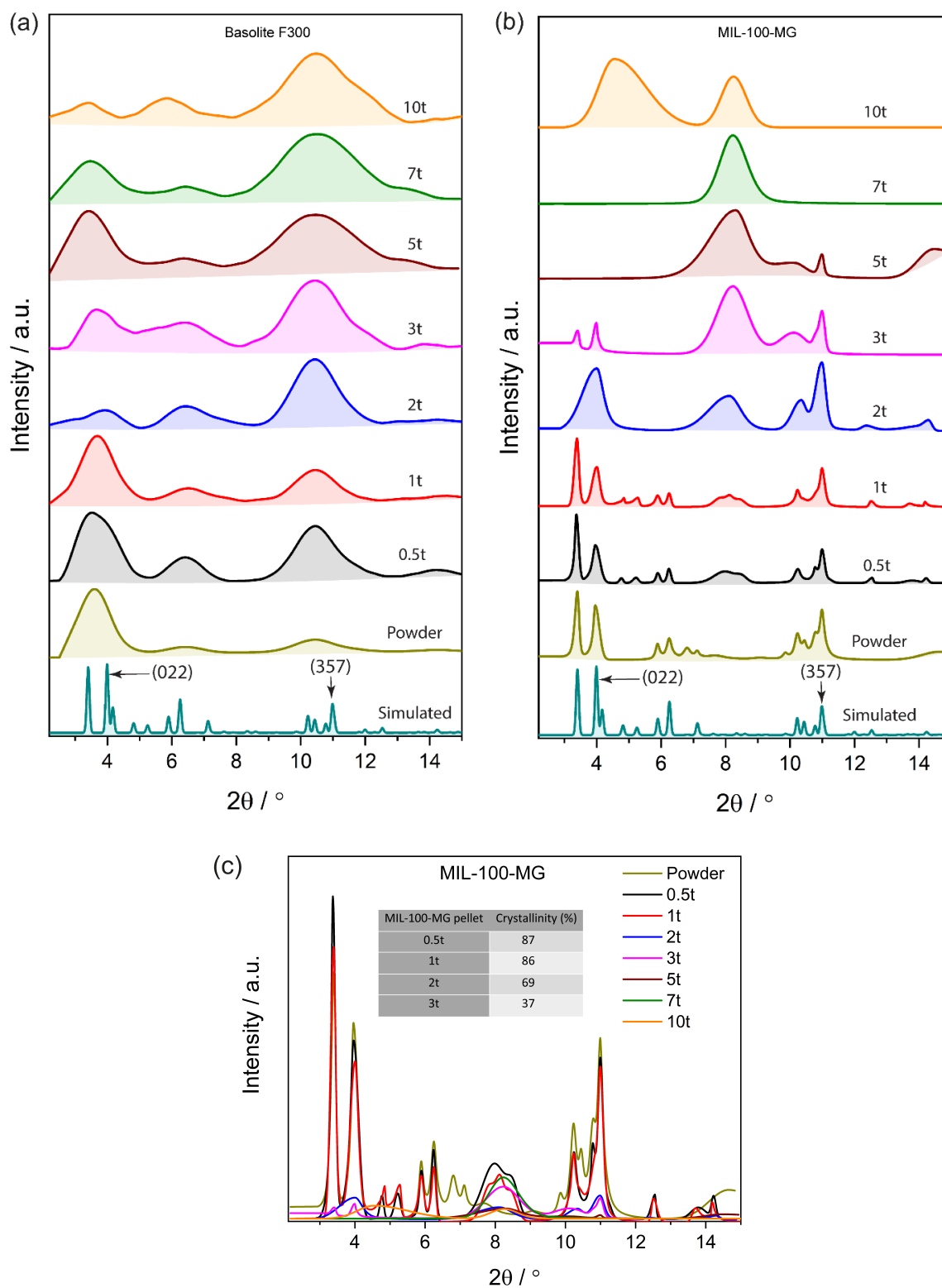
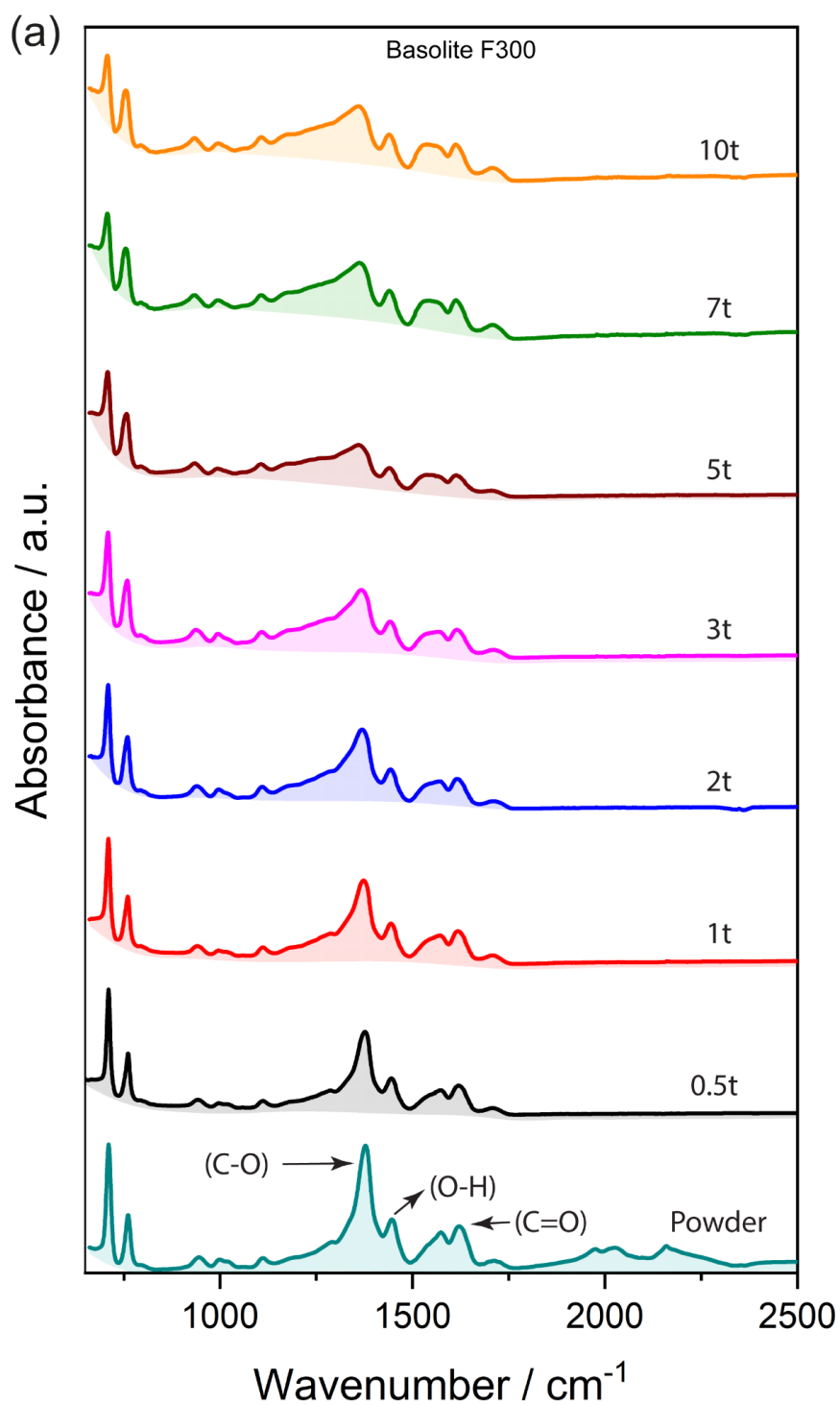


Figure S1: The XRD patterns for: (a) Basolite F300 and (b) MIL-100-MG pellets, both normalized with respect to the highest data point. (c) XRD patterns in absolute intensities for

MIL-100-MG pellets. Inset of table shows the pellet crystallinity (%), estimated from the area ratio of the crystalline peaks to the total area found under the XRD pattern.

2. Fourier-transform infrared spectroscopy (ATR-FTIR)



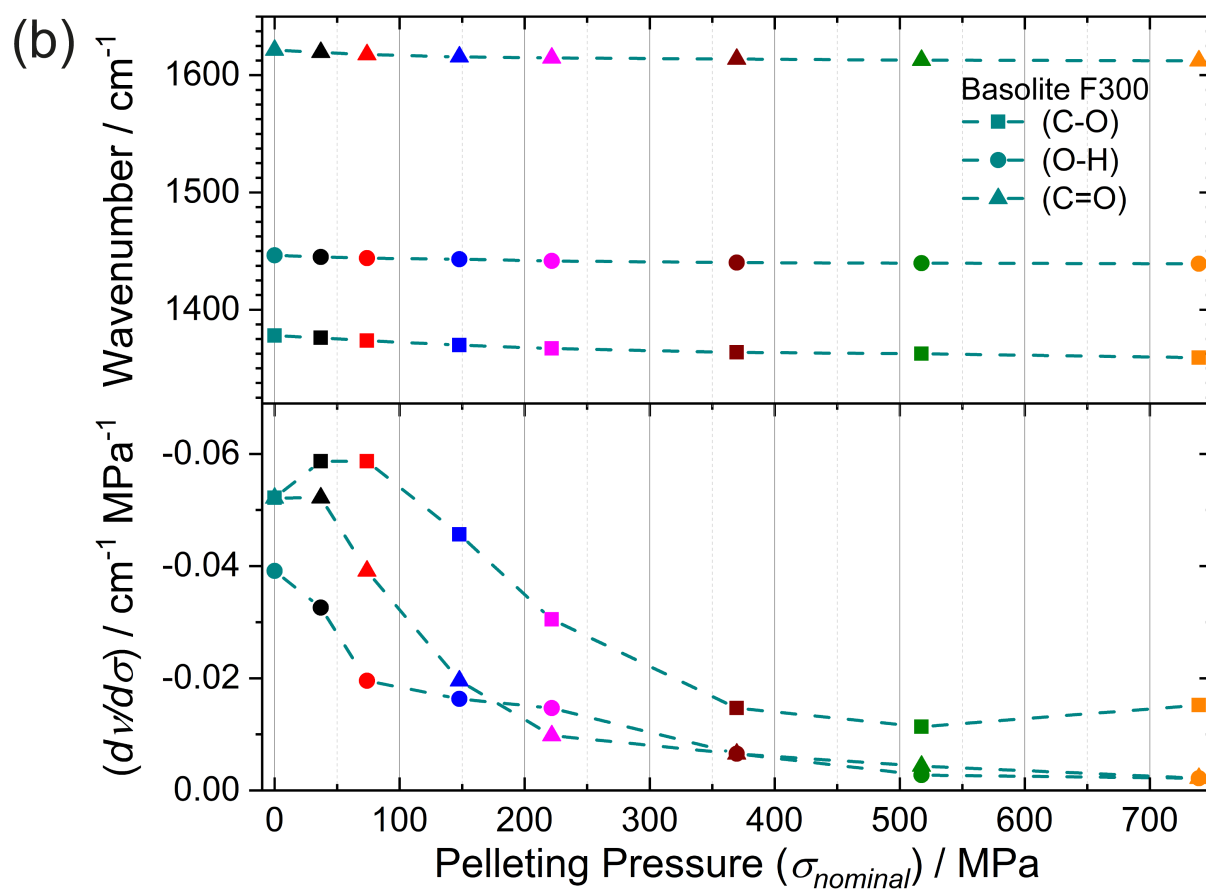


Figure S2: (a) The pressure-dependent ATR-FTIR spectra for Basolite F300 pellets, (b) Derivative of peak shift over pelleting pressure.

3. Thermogravimetric analysis (TGA)

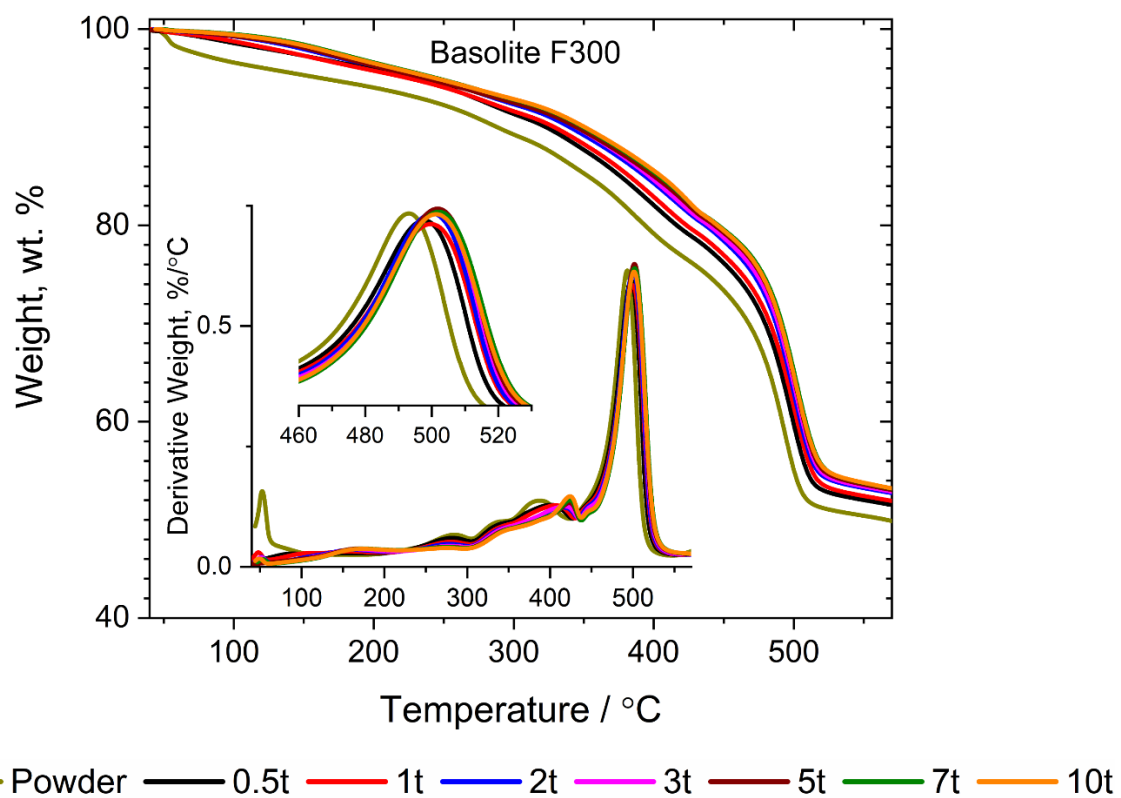
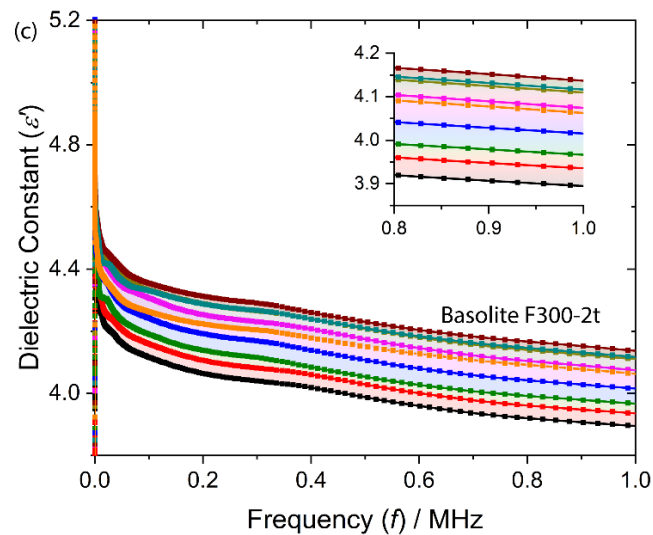
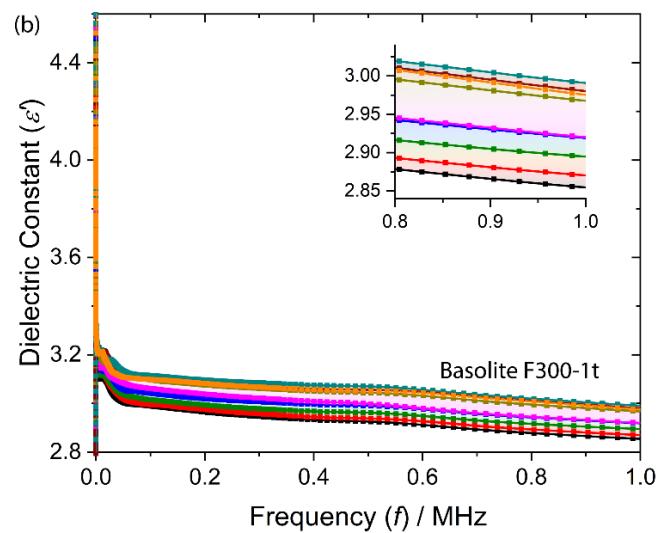
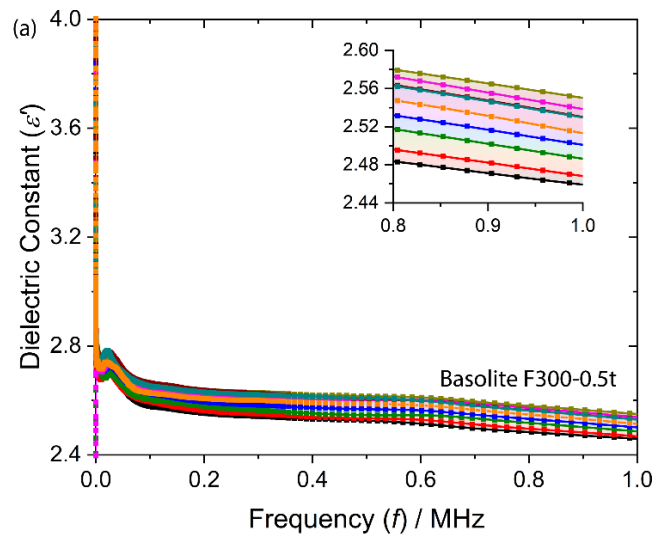


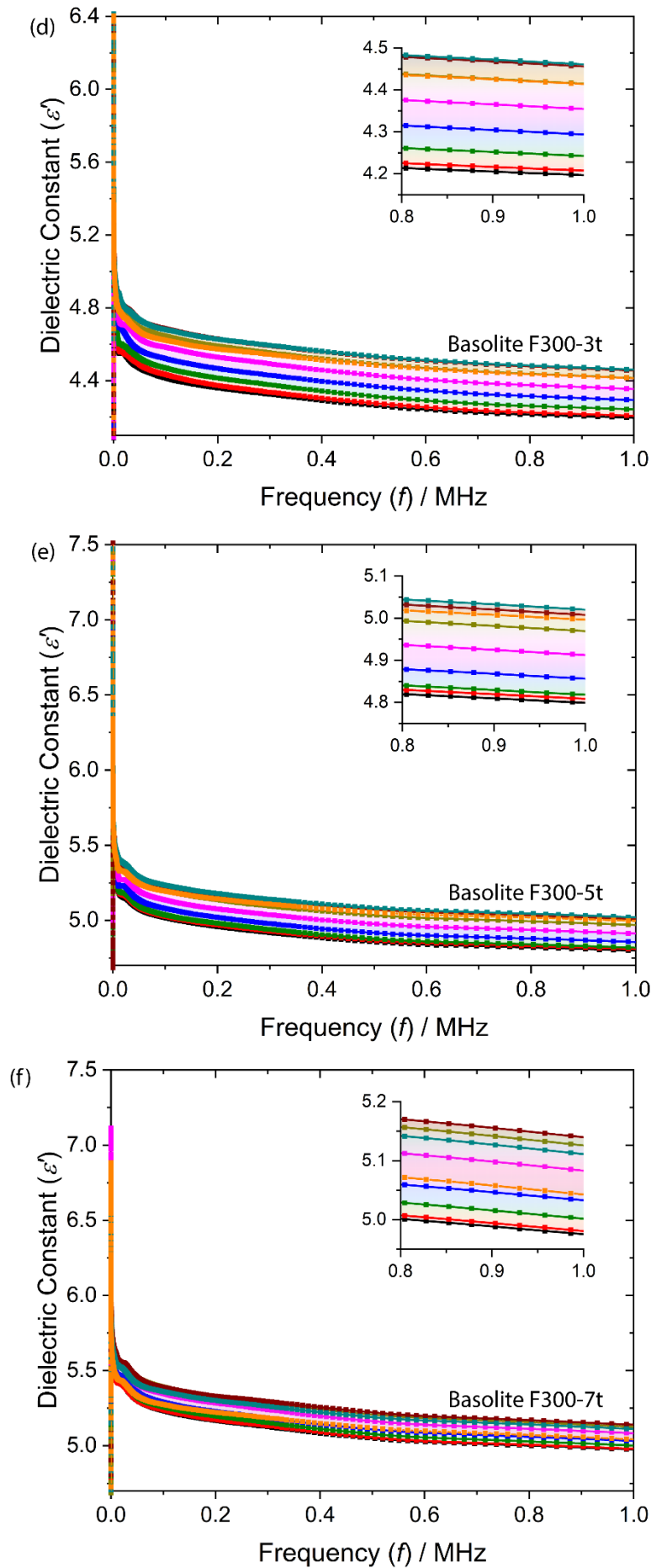
Figure S3: The pressure-dependent thermal stability measurement (TGA) for Basolite F300 pellets.

4. Dielectric properties

4.1 Basolite F300

4.1.1 Real Part of Dielectric Constant (ϵ')





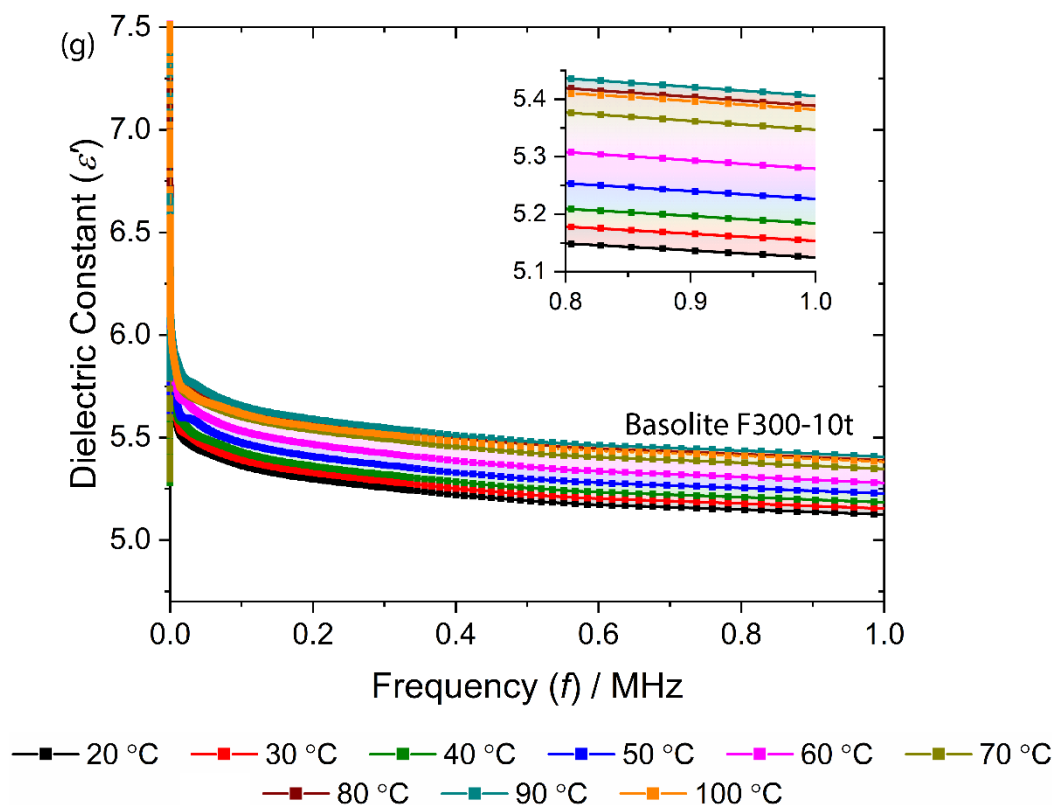
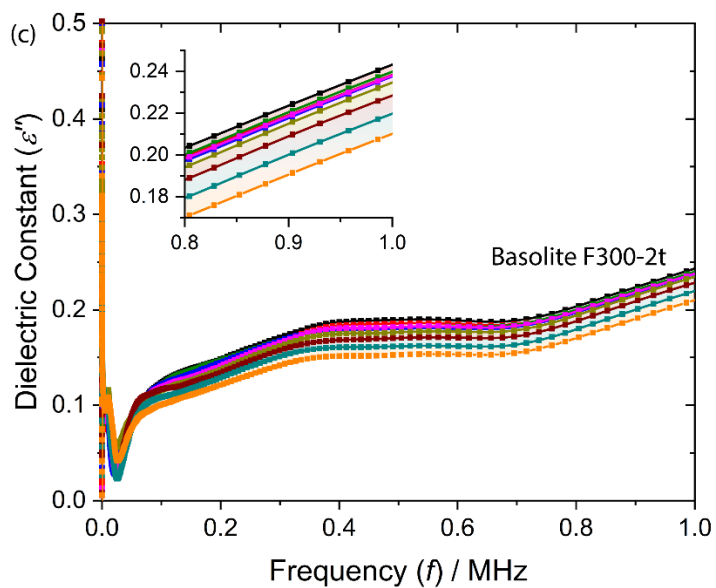
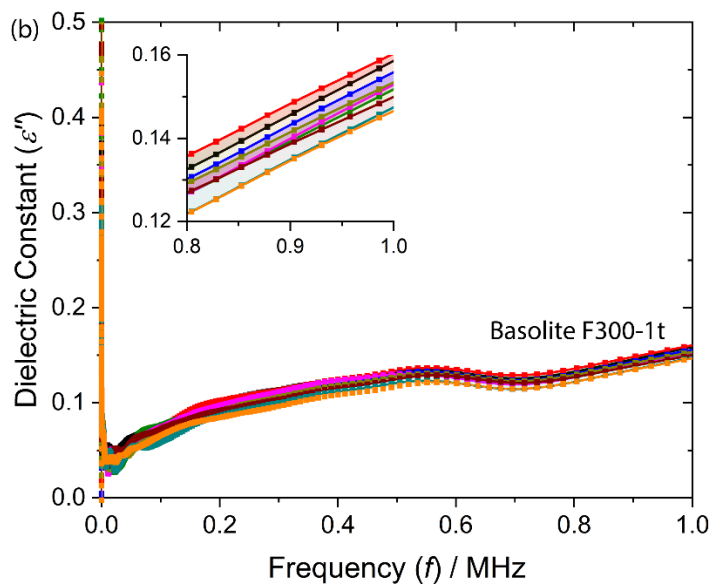
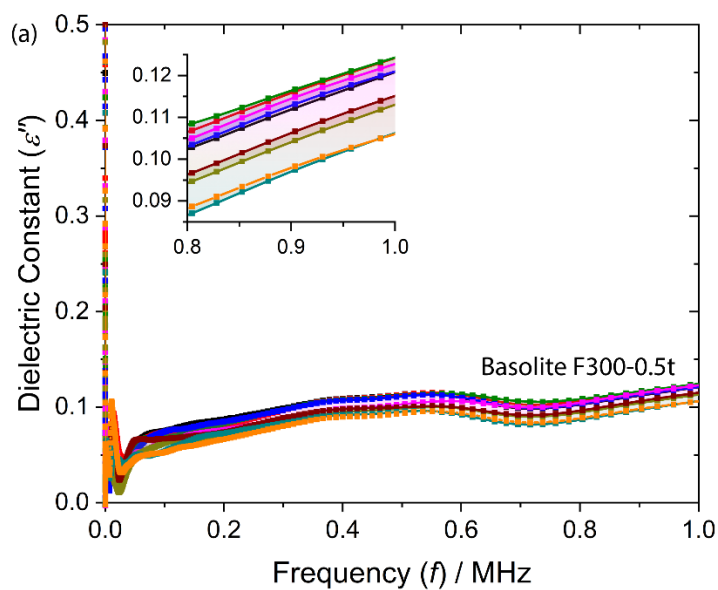
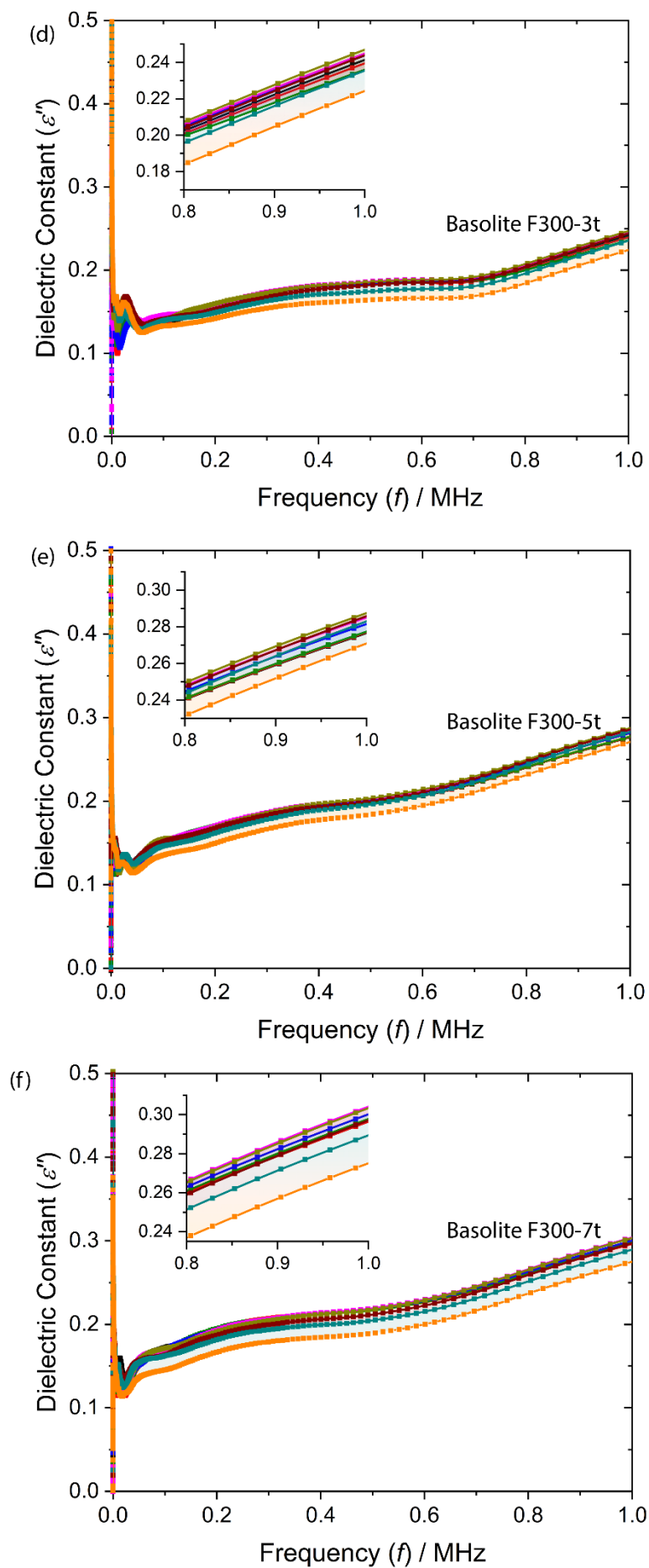


Figure S4: The real part of dielectric constant for Basolite F300 pellets prepared under a compression load of: (a) 0.5-ton, (b) 1-ton, (c) 2-ton, (d) 3-ton (e) 5-ton (f) 7-ton, and (g) 10-ton, corresponding to the pressure of 36.96, 73.92, 147.84, 221.76, 369.6, 517.44 and 739.20 MPa, respectively.

4.1.2 Imaginary Part of Dielectric Constant (ϵ'')



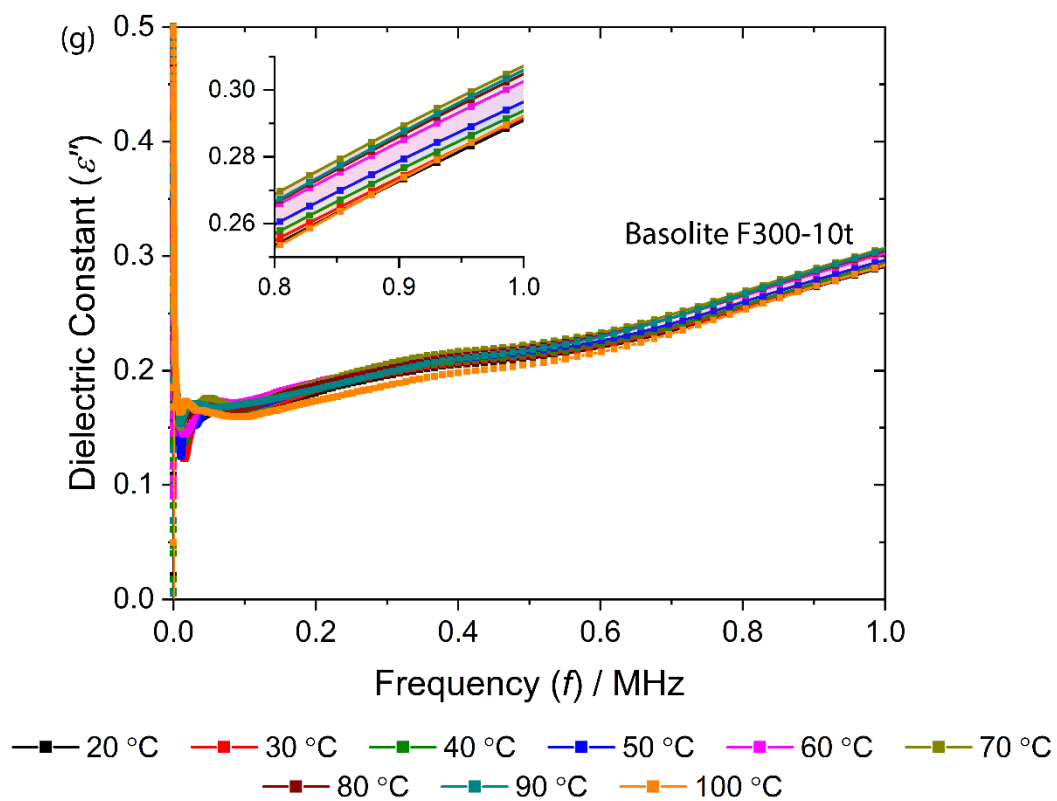
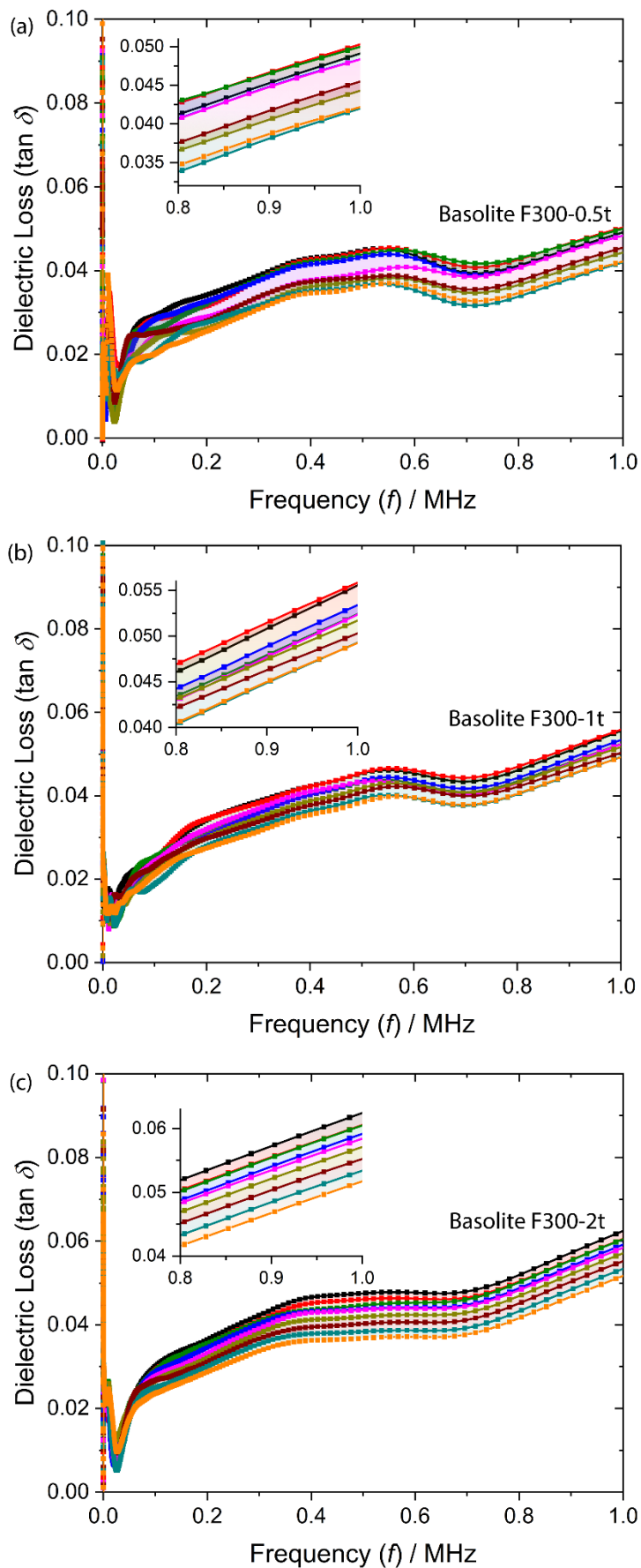
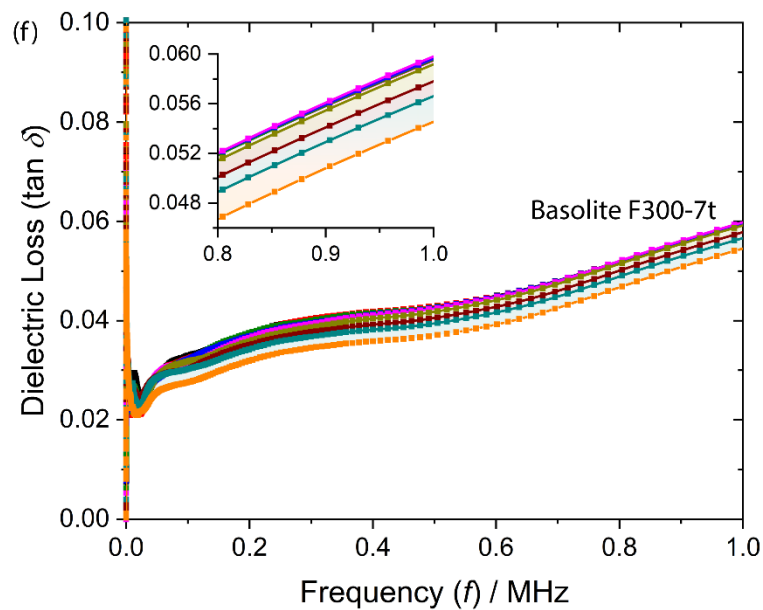
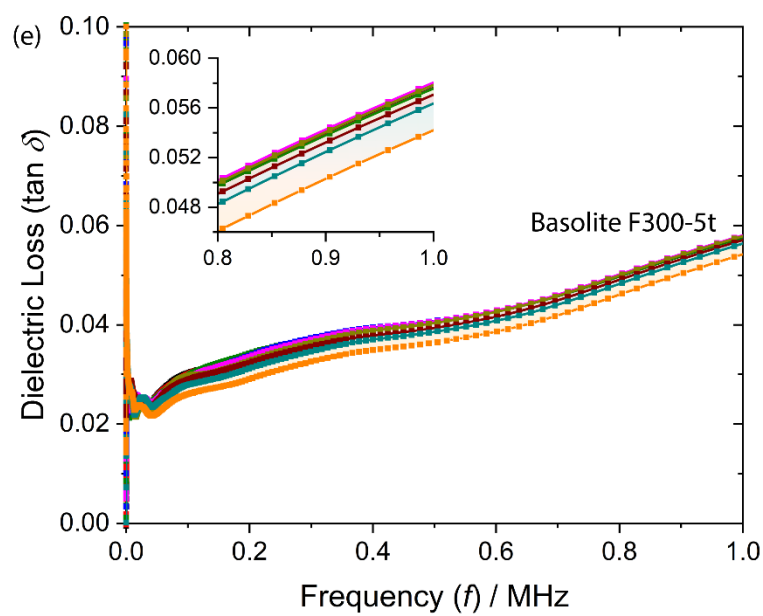
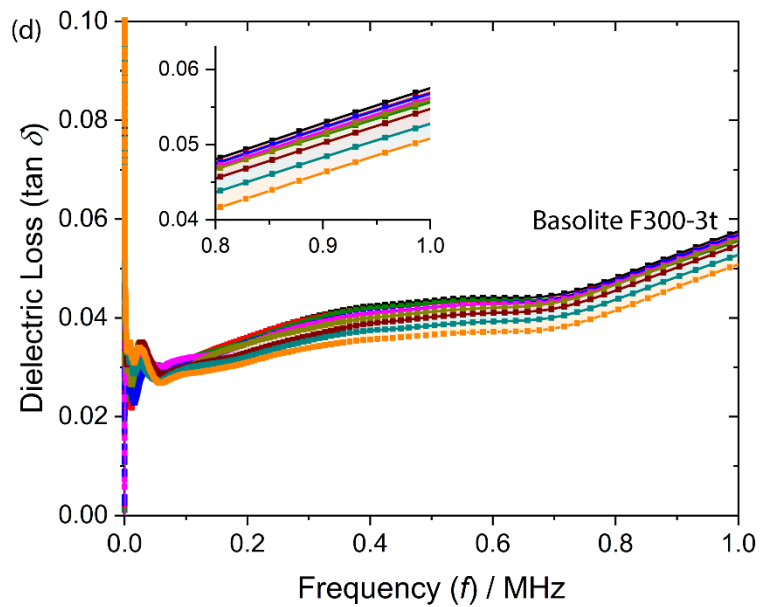


Figure S5: The imaginary part of dielectric constant for Basolite F300 pellets prepared under a compression load of: (a) 0.5-ton, (b) 1-ton, (c) 2-ton, (d) 3-ton (e) 5-ton (f) 7-ton, and (g) 10-ton, respectively.

4.1.3 Dielectric Loss ($\tan \delta$)



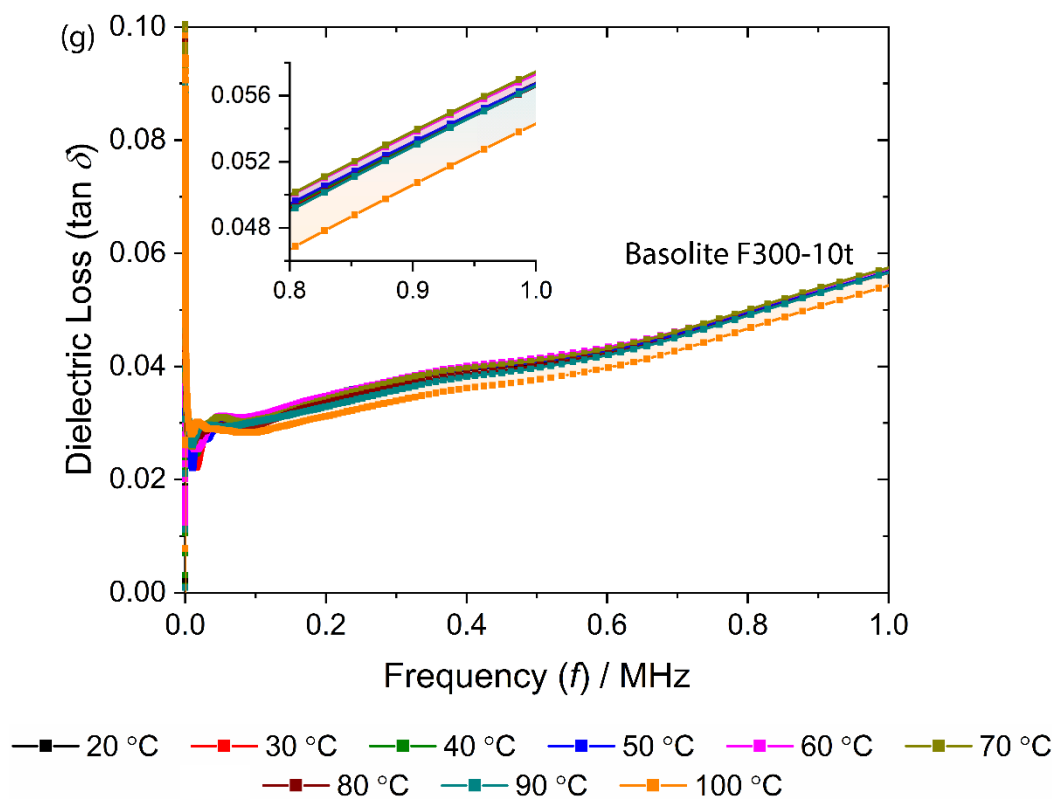
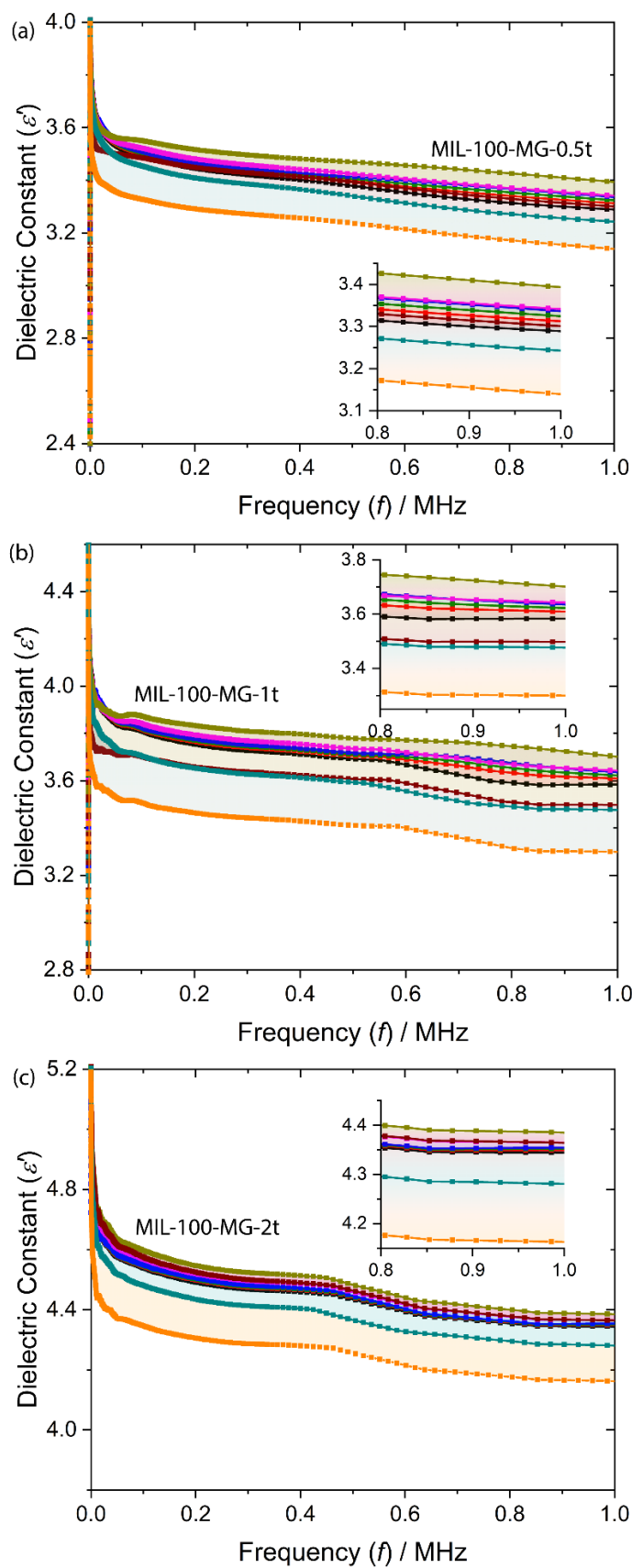
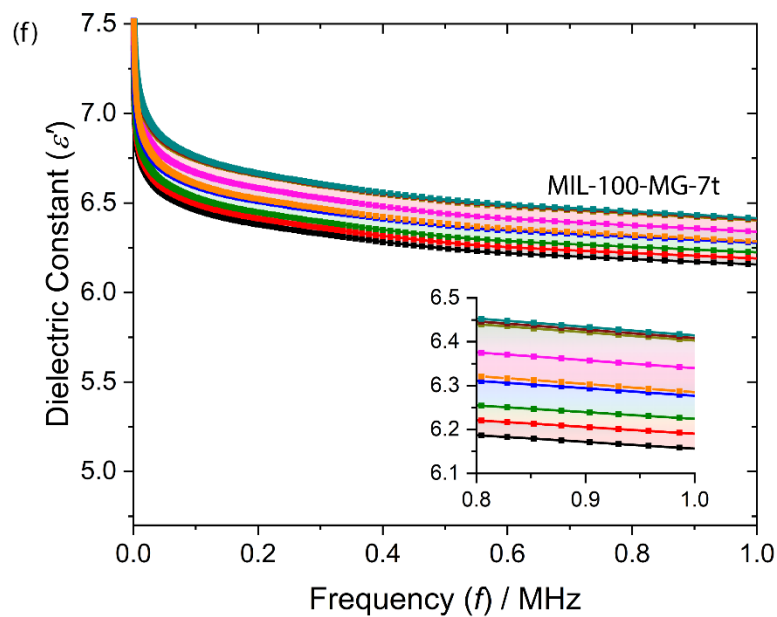
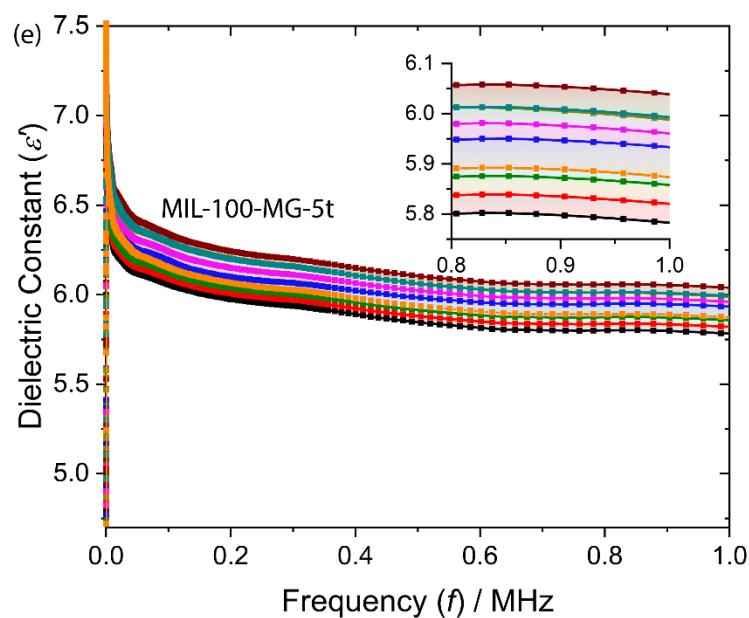
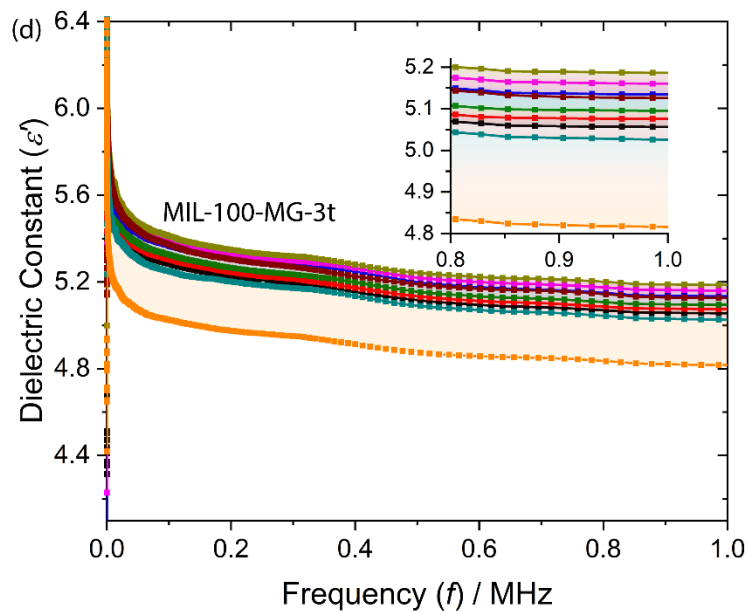


Figure S6: The dielectric loss for Basolite F300 pellets prepared under a compression load of: (a) 0.5-ton, (b) 1-ton, (c) 2-ton, (d) 3-ton (e) 5-ton (f) 7-ton, and (g) 10-ton, respectively.

4.2 MIL-100-MG

4.2.1 Real Part of Dielectric Constant





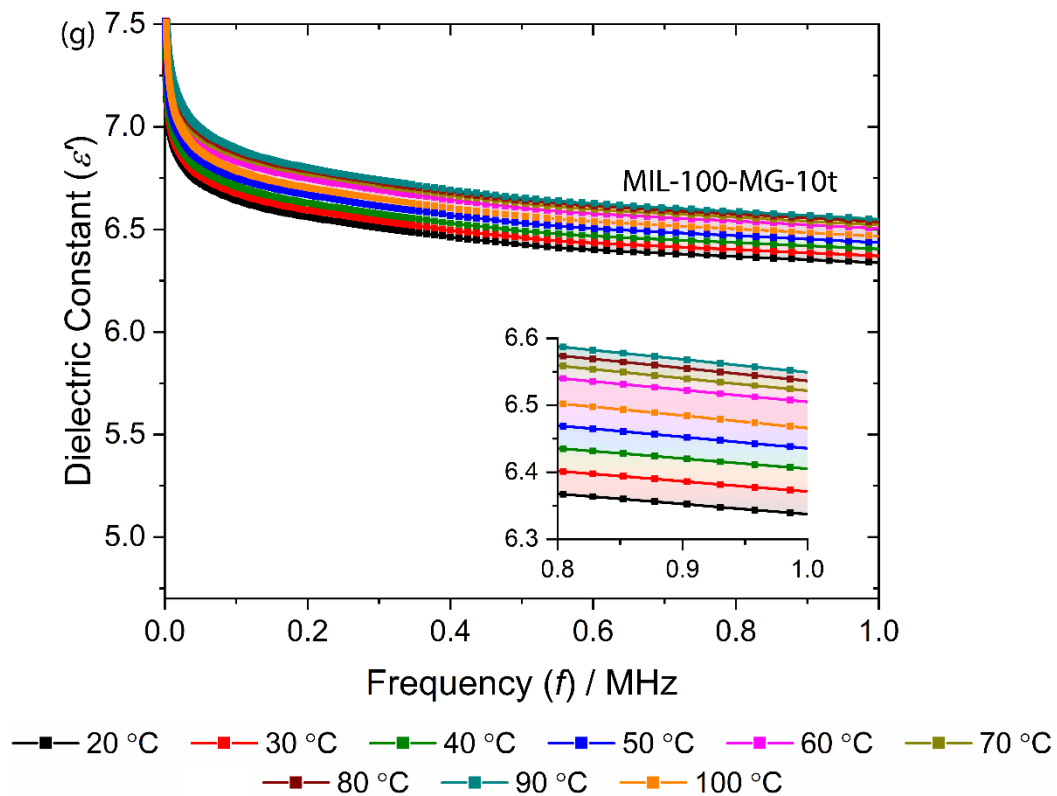
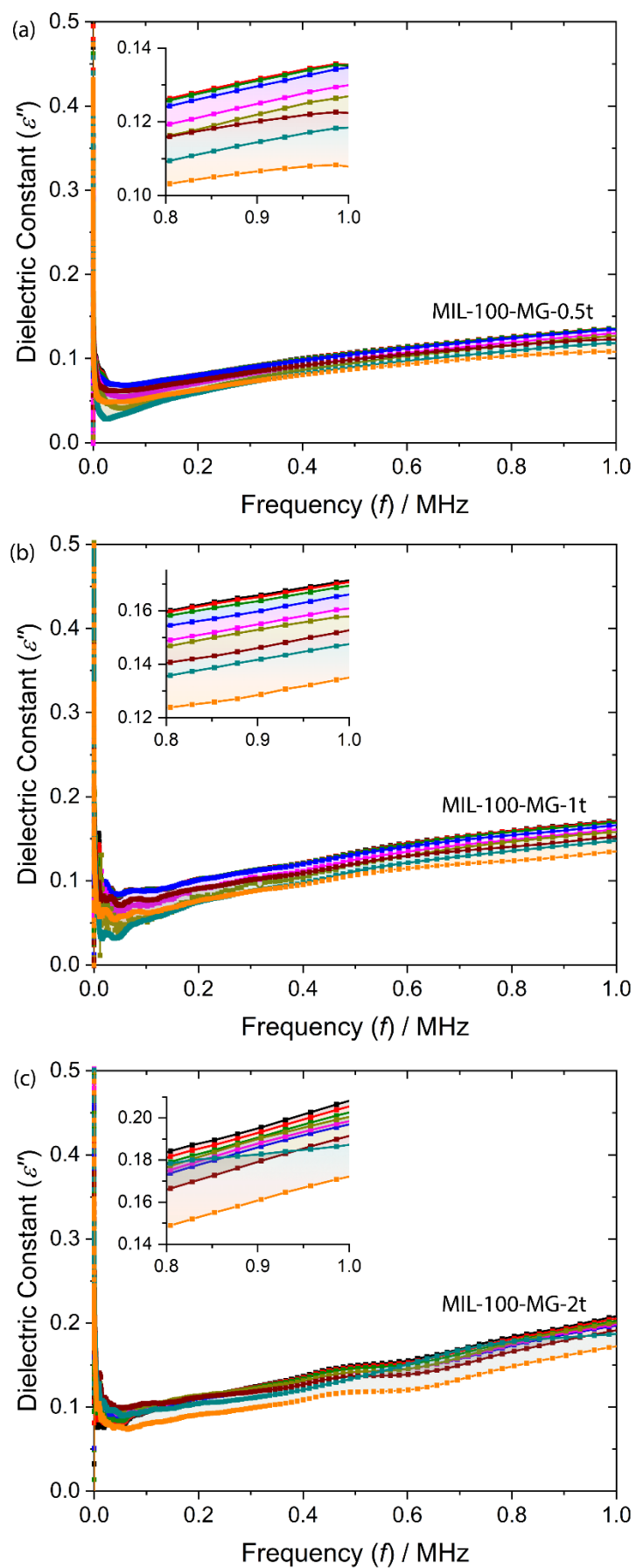
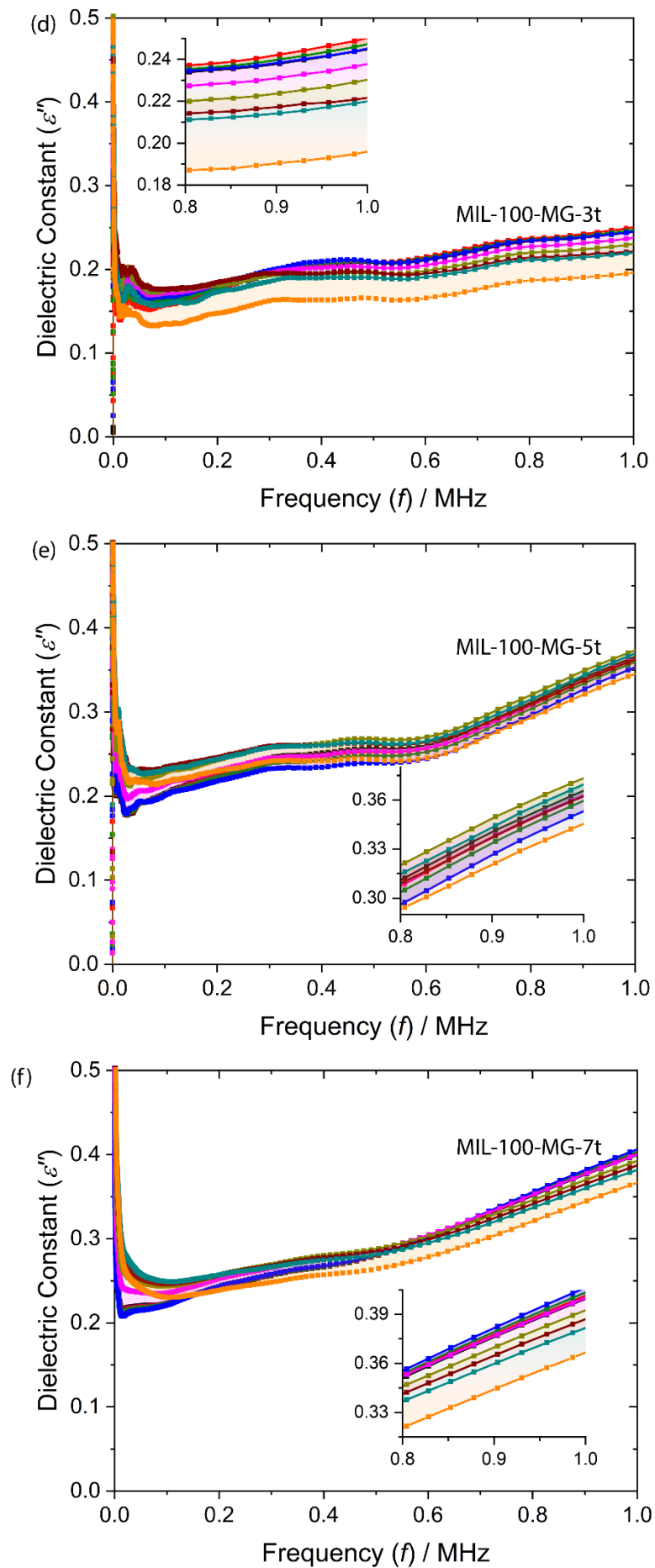


Figure S7: The real part of dielectric constant for MIL-100-MG pellets prepared under a compression load of: (a) 0.5-ton, (b) 1-ton, (c) 2-ton, (d) 3-ton (e) 5-ton (f) 7-ton, and (g) 10-ton, corresponding to the pressure of 36.96, 73.92, 147.84, 221.76, 369.6, 517.44 and 739.20 MPa, respectively.

4.2.2 Imaginary Part of Dielectric Constant





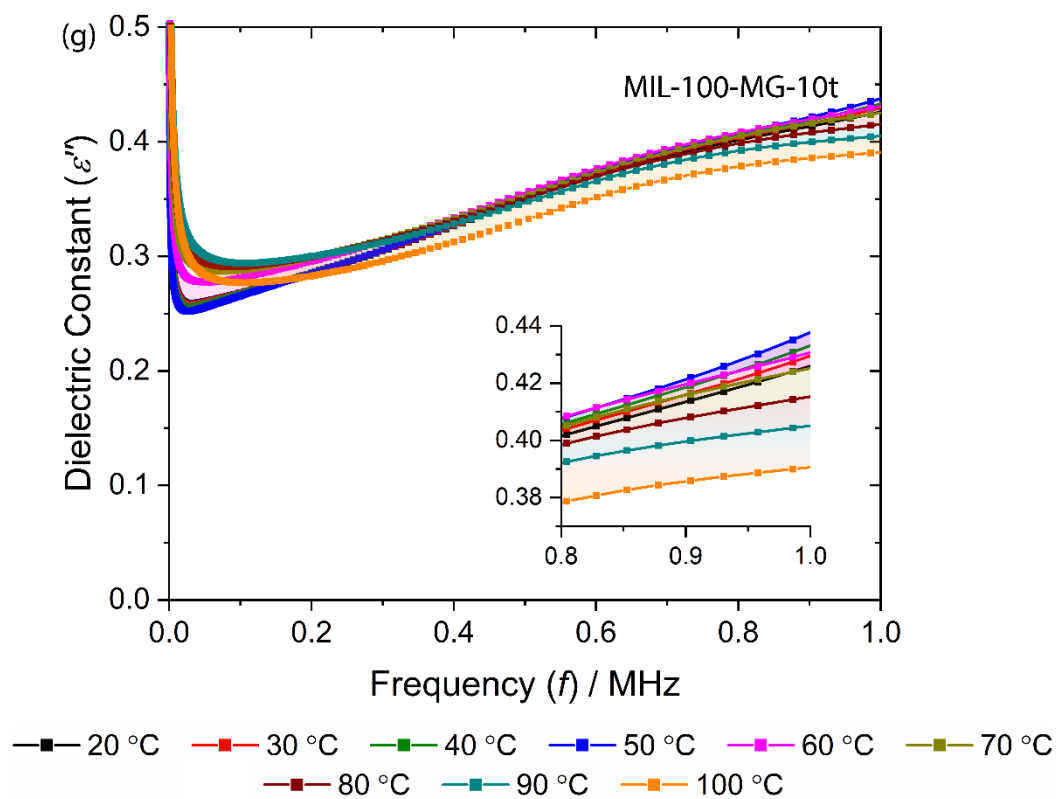
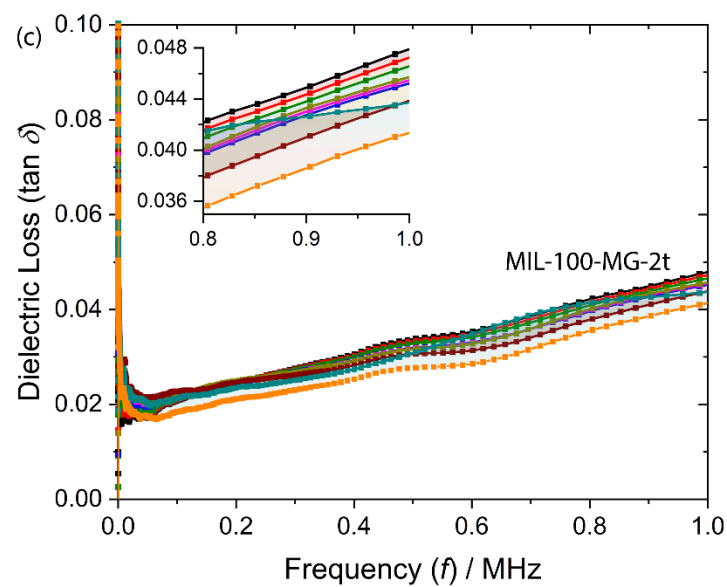
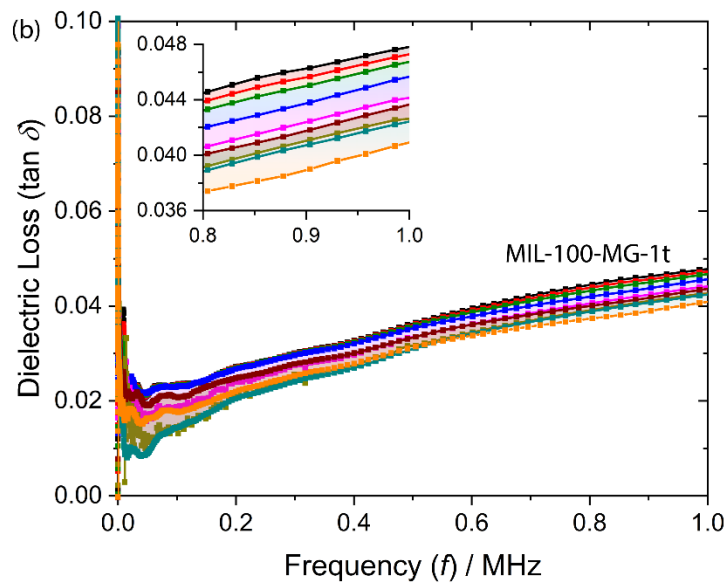
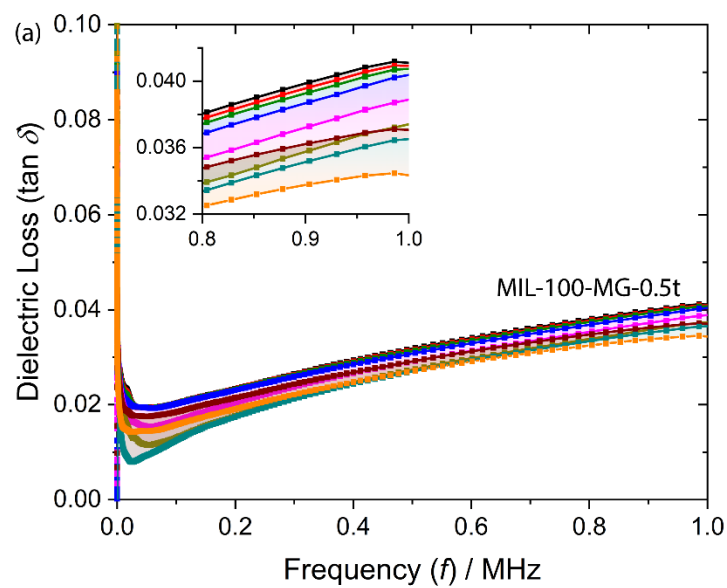
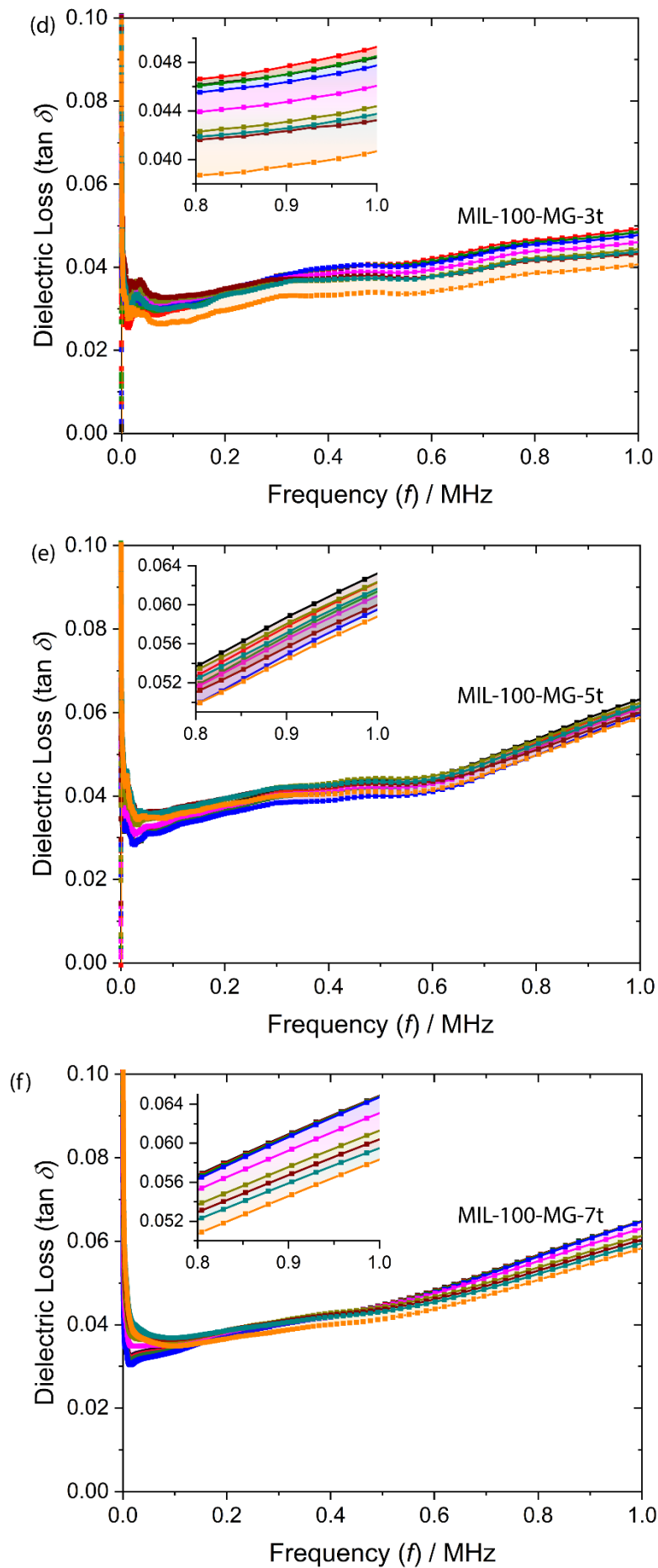


Figure S8: The imaginary part of dielectric constant for MIL-100-MG pellets prepared under a compression load of: (a) 0.5-ton, (b) 1-ton, (c) 2-ton, (d) 3-ton (e) 5-ton (f) 7-ton, and (g) 10-ton, respectively.

4.2.3 Dielectric Loss





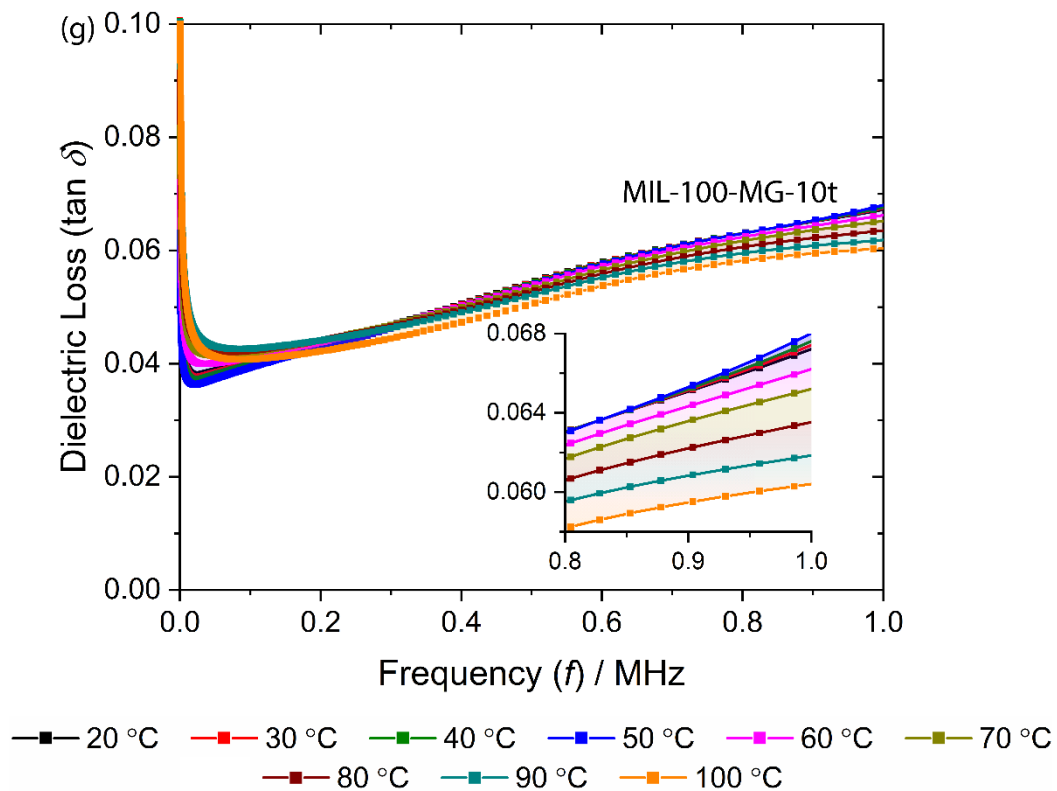


Figure S9: The dielectric loss for MIL-100-MG pellets prepared under a compression load of: (a) 0.5-ton, (b) 1-ton, (c) 2-ton, (d) 3-ton (e) 5-ton (f) 7-ton, and (g) 10-ton, respectively.

4.3 Comparative dielectric loss

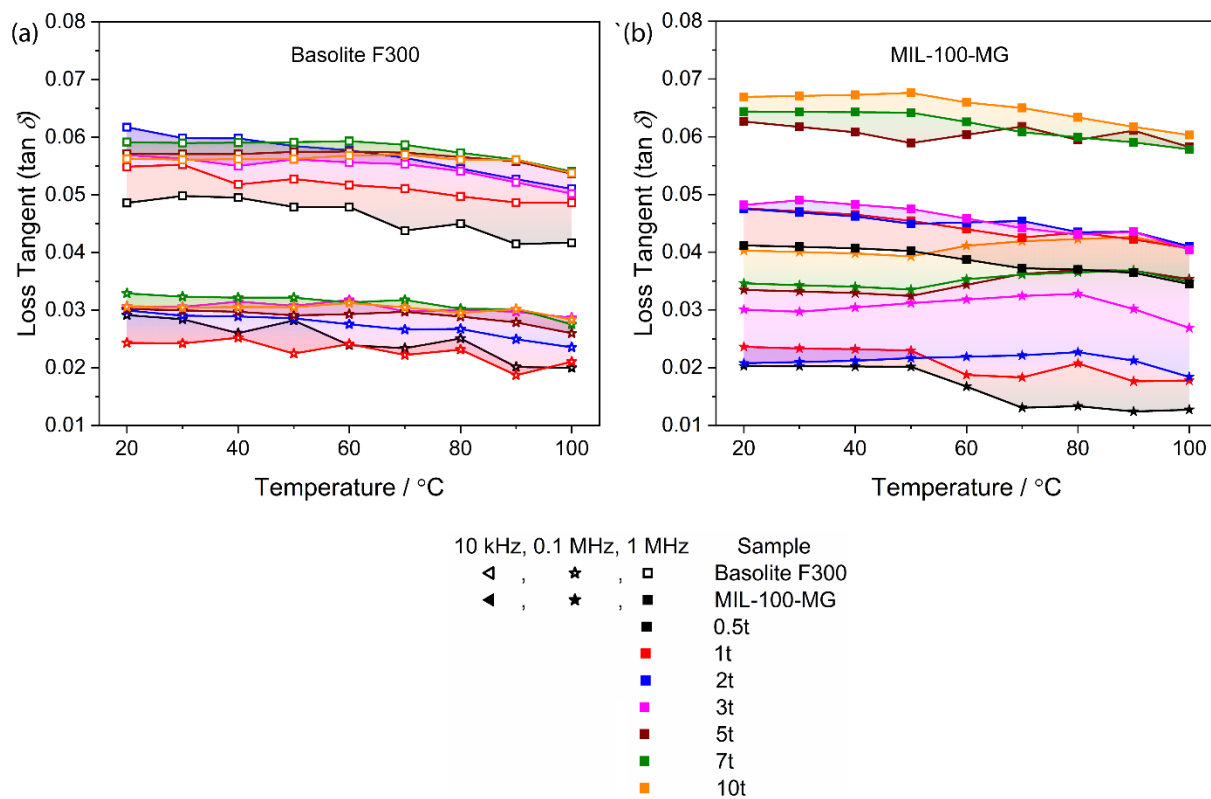


Figure S10: Dielectric loss of MOF pellets as a function of pelleting pressure and temperature:

(a) Basolite F300 and, (b) MIL-100-MG pellets specific frequencies (0.01, 0.1, and 1 MHz).

5. Reflectivity spectra $R(\omega)$ in the far-IR and mid-IR regions

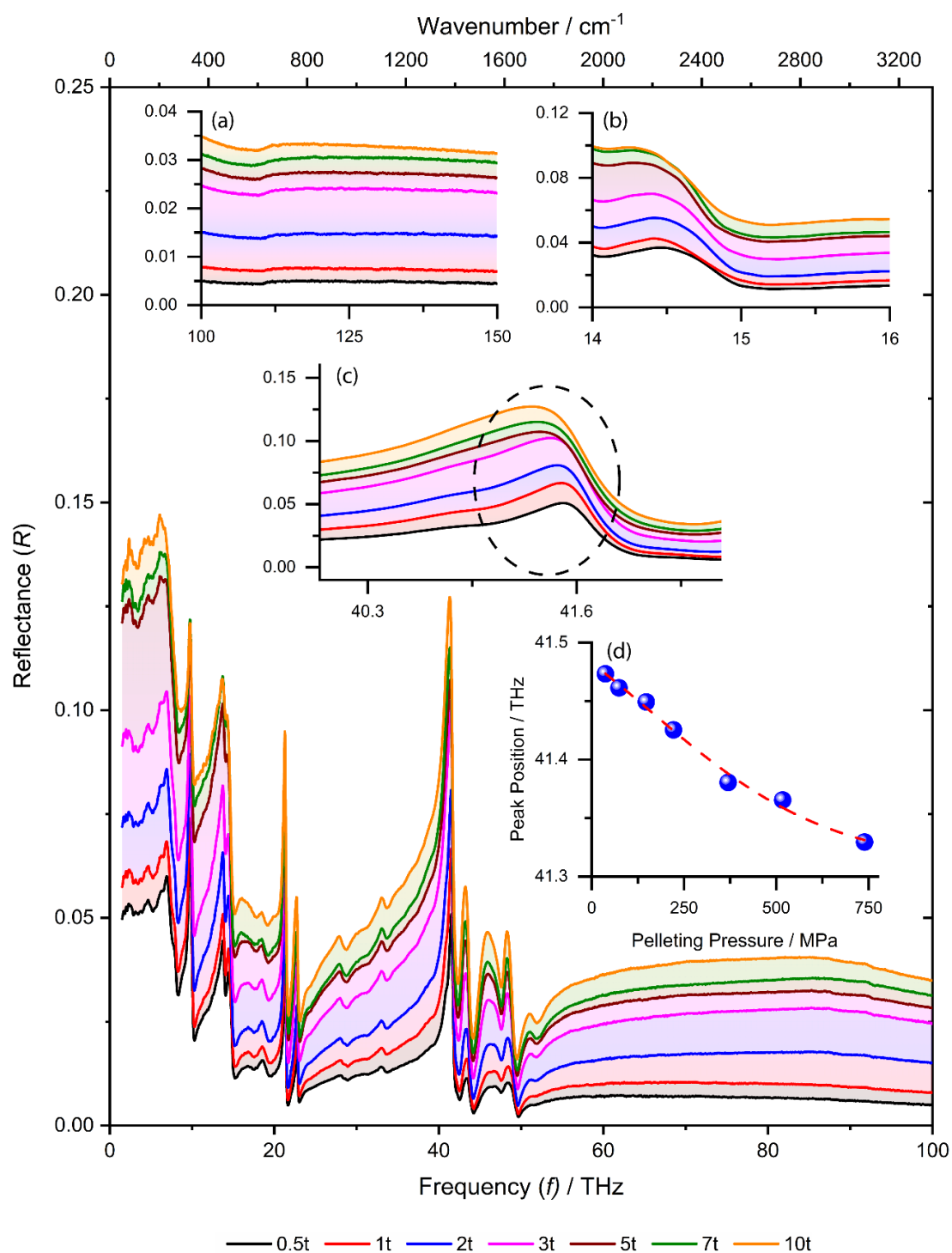


Figure S11: Reflectance spectra of MIL-100-MG pellets. Inset: (a) reflectivity spectra in the near-IR region, (b) joining of the far-IR and mid-IR spectra at 517 cm^{-1} (~ 15.5 THz), (c) pelleting pressure-dependent redshift in transition mode of peaks obtained from the Gaussian peak fitting and (d) plot for pressure-dependent peak shift in peak positions.

6. Refractive index in THz region

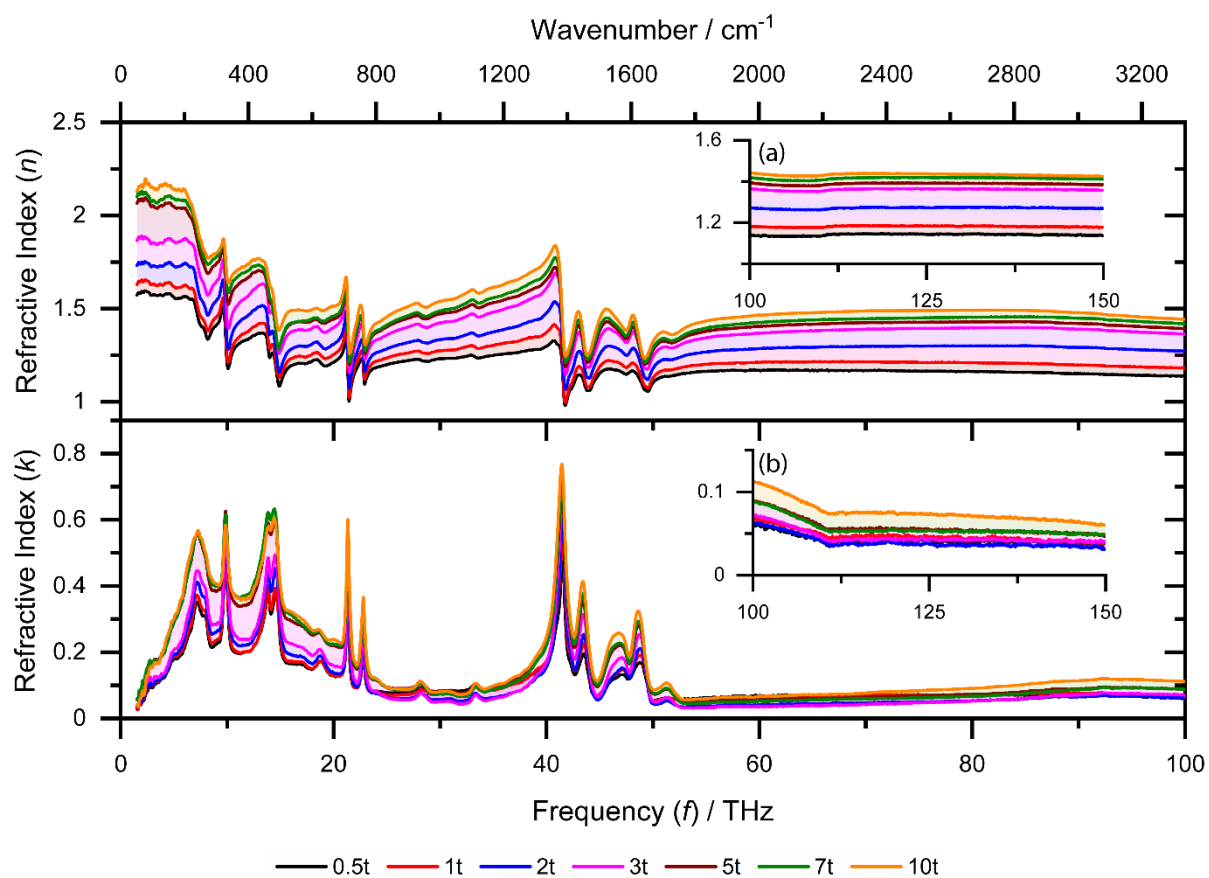


Figure S12: (a) Real and (b) imaginary parts of the refractive index of MIL-100 pellets in IR frequency range. Inset (c)-(d) shows the optically insensitivity of the framework in near-IR region.

7. The imaginary part of dielectric constant in the THz region

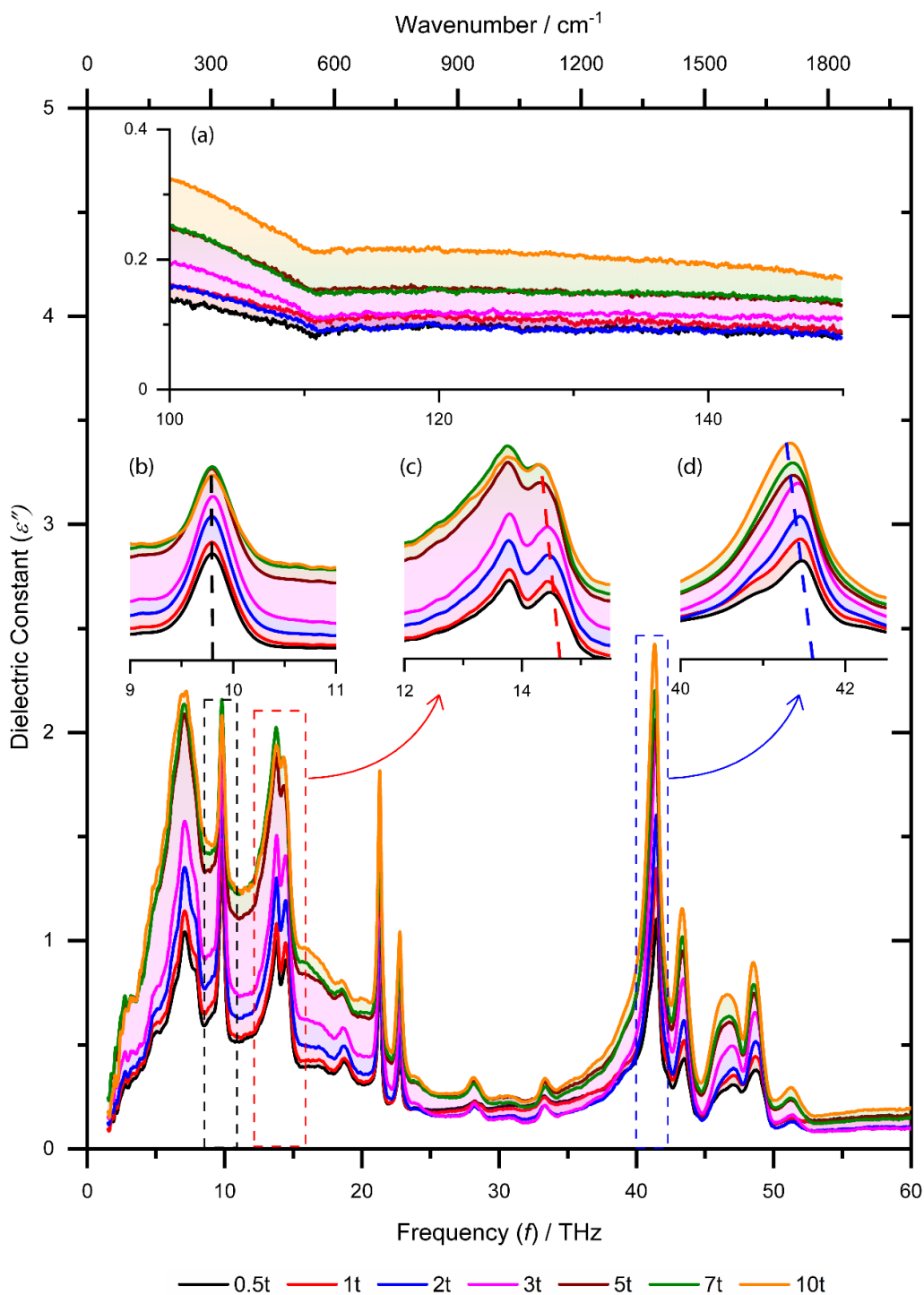
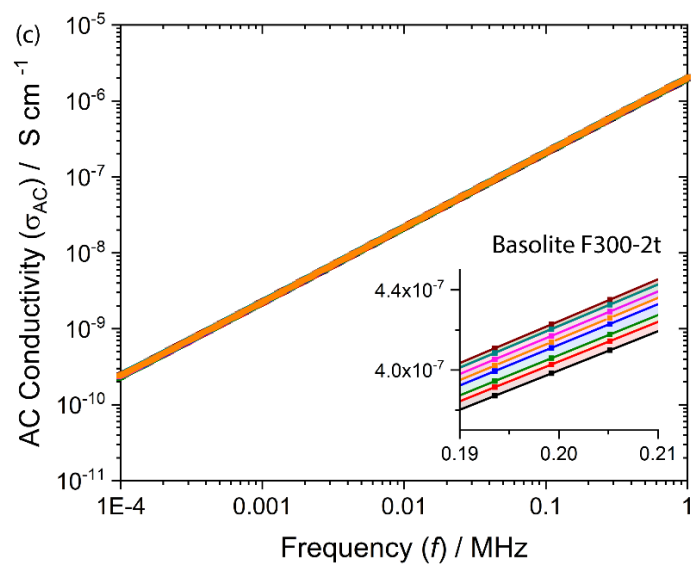
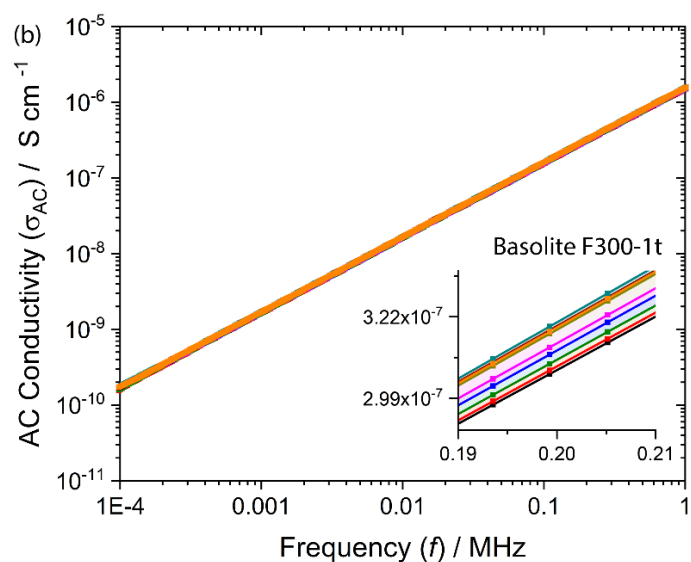
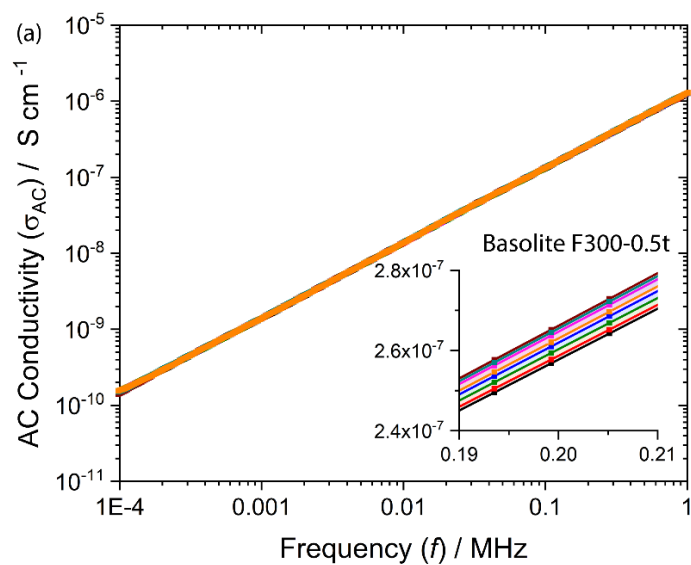
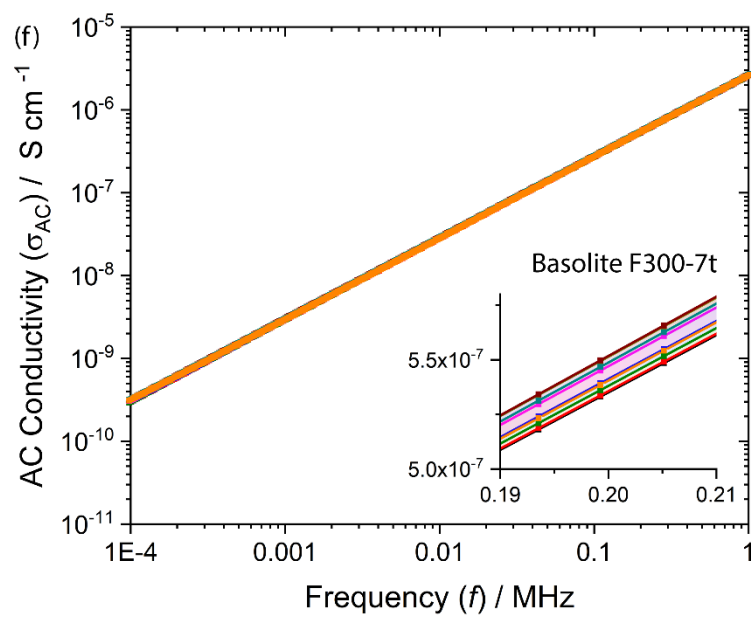
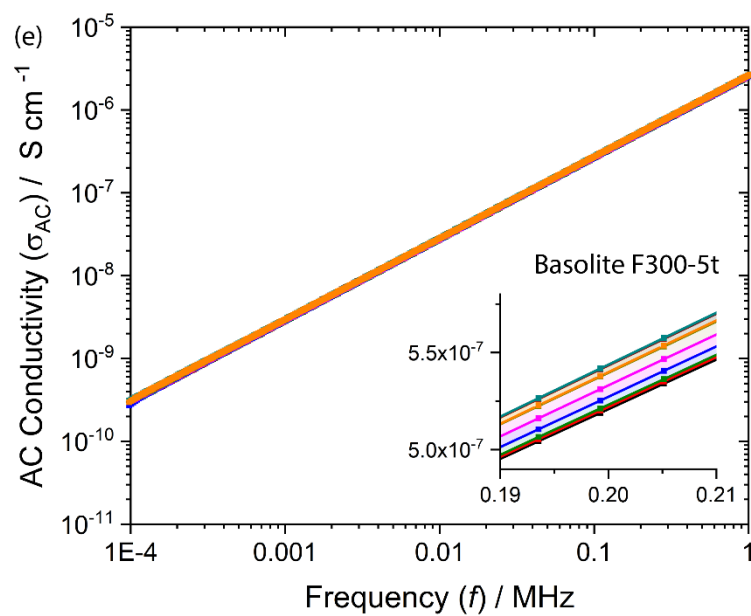
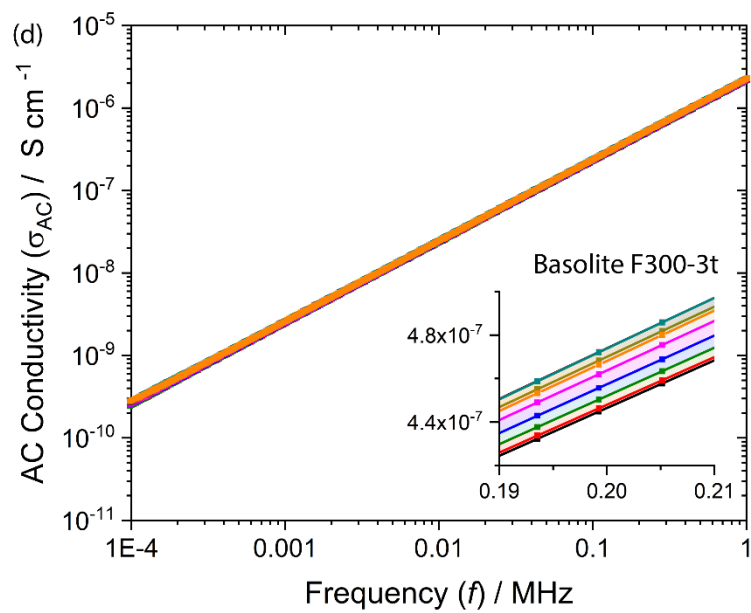


Figure S13: The imaginary part of dielectric constant (ϵ'') in the IR frequency range for MIL-100 pellets. Inset (a) shows the ϵ'' spectrum in the near-IR region. Inset (b) doesn't show any shift in the transition mode, whereas, in inset (c)-(d) the redshift is evident in the transition modes caused by the pelleting force-induced amorphization.

8. AC conductivity

8.1 Basolite F300





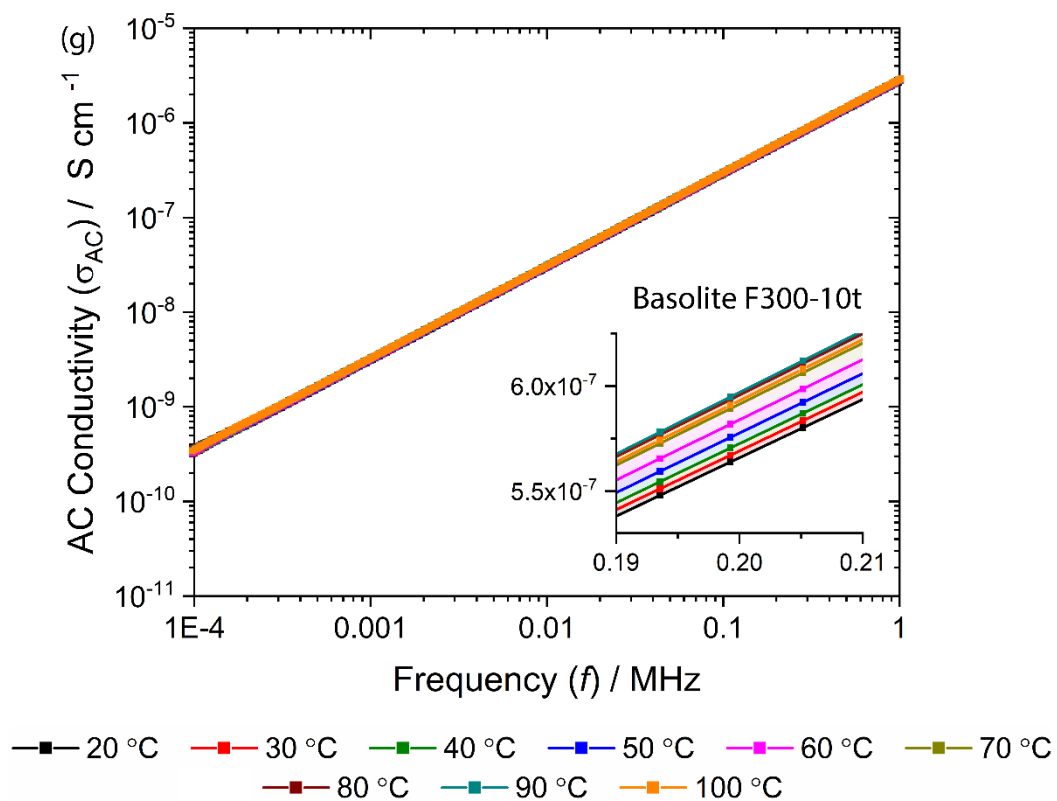
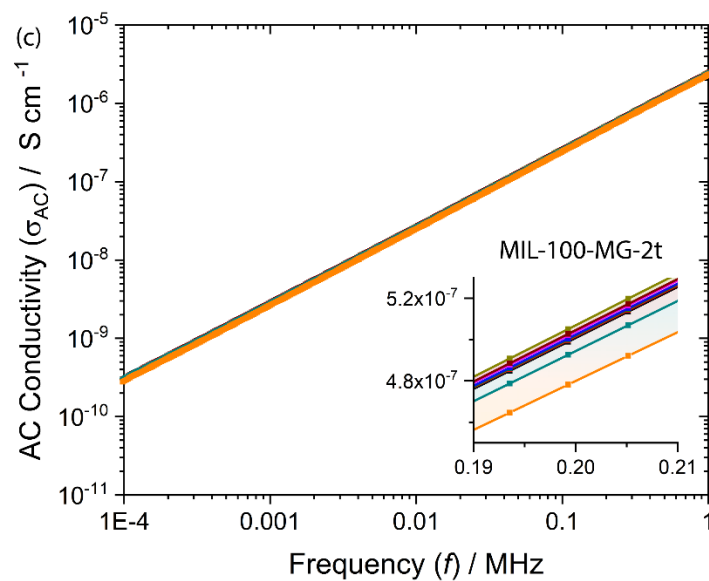
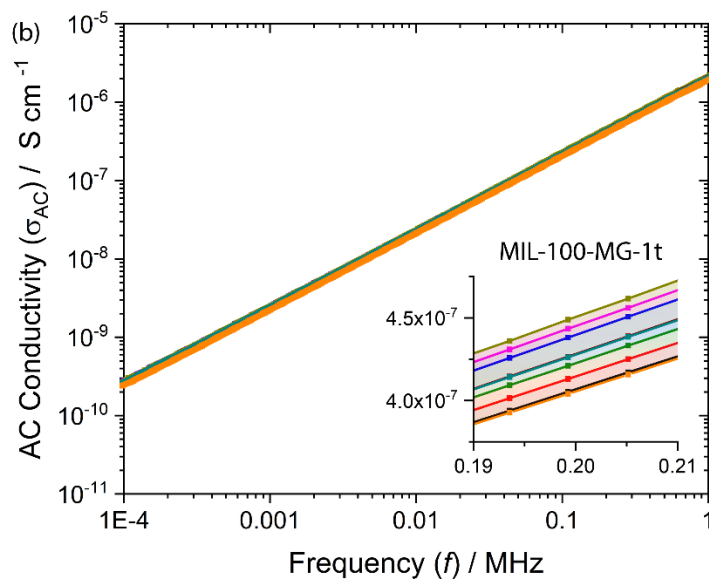
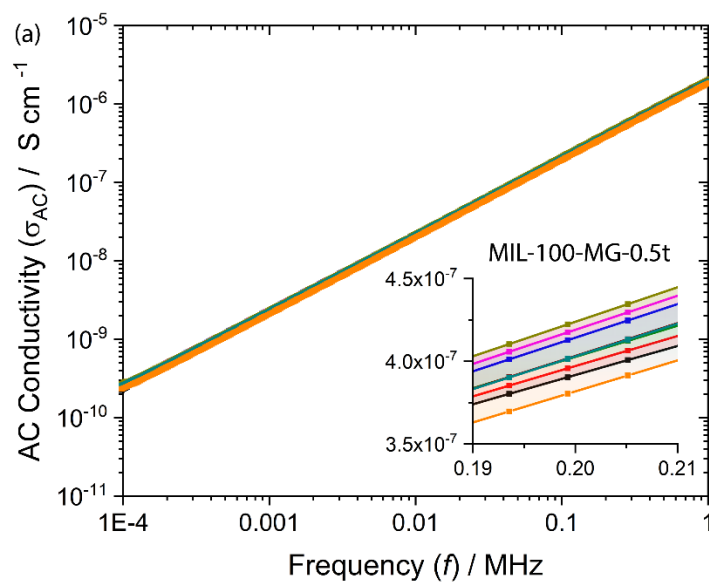
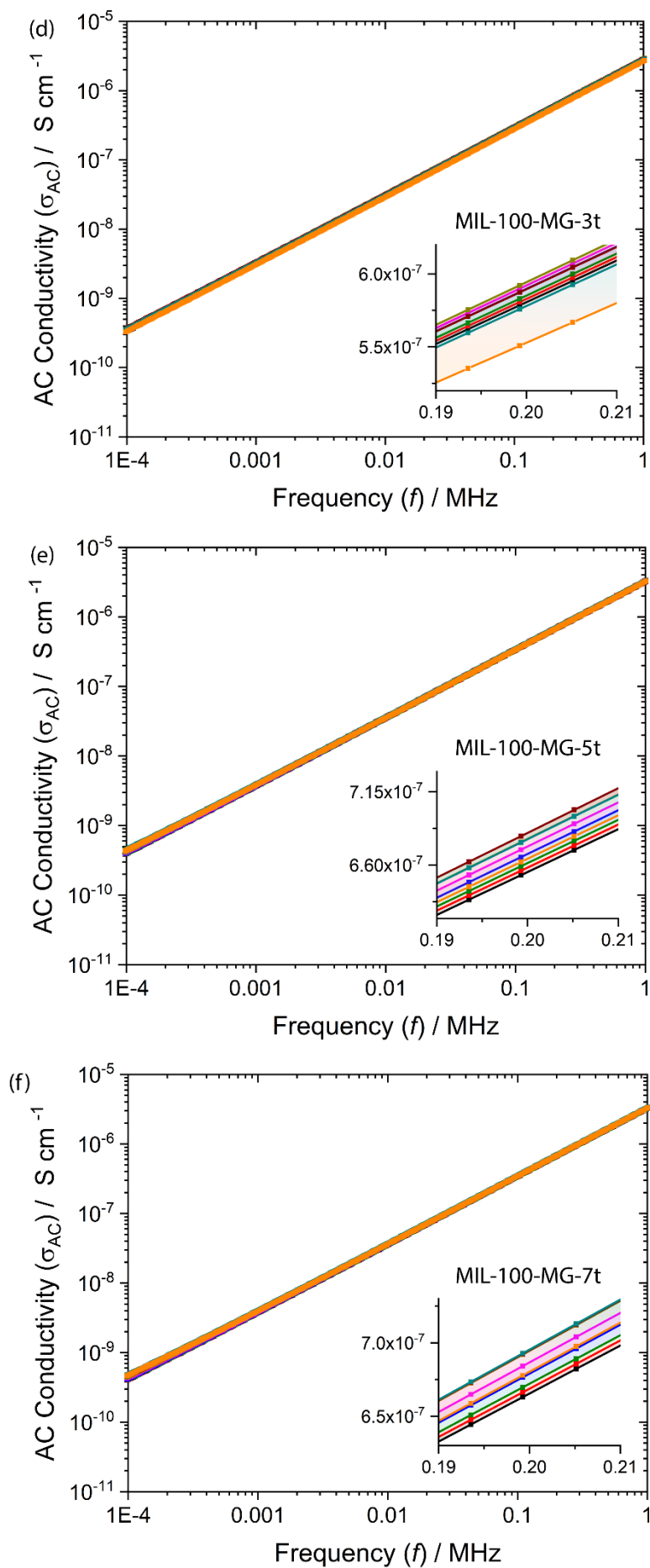


Figure S14: The AC conductivity of Basolite F300 pellets prepared under a compression load of: (a) 0.5-ton, (b) 1-ton, (c) 2-ton, (d) 3-ton (e) 5-ton (f) 7-ton, and (g) 10-ton, corresponding to the pressure of 36.96, 73.92, 147.84, 221.76, 369.6, 517.44 and 739.20 MPa, respectively.

8.2 MIL-100-MG





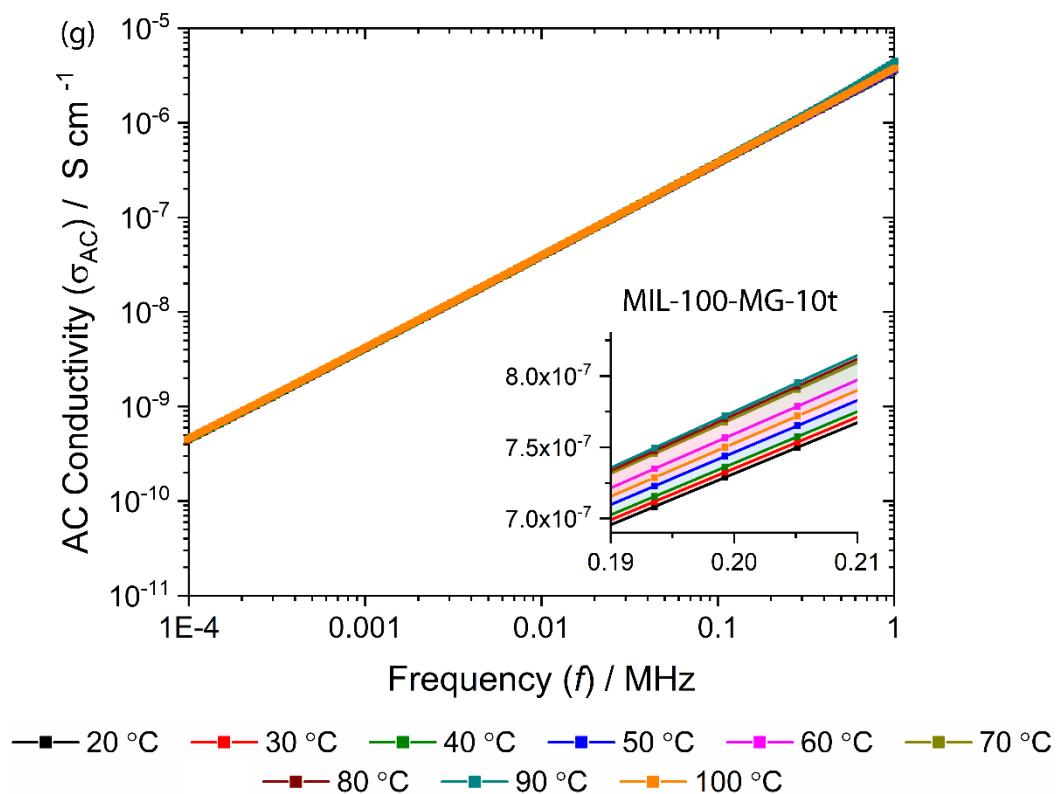


Figure S15: The AC conductivity of MIL-100-MG pellets prepared under a compression load of: (a) 0.5-ton, (b) 1-ton, (c) 2-ton, (d) 3-ton (e) 5-ton (f) 7-ton, and (g) 10-ton, corresponding to the pressure of 36.96, 73.92, 147.84, 221.76, 369.6, 517.44 and 739.20 MPa, respectively.